SYSTEMS ANALYSIS OF A MICROFABRICATED STORABLE BIPROPELLANT ROCKET ENGINE

by

CHRISTOPHER S. PROTZ

S. B. Aeronautics and Astronautics
Massachusetts Institute of Technology, 1998

Submitted to the Department of Aeronautics and Astronautics
in partial fulfillment of the requirements for the degree of

MASTER OF SCIENCE IN AERONAUTICS AND ASTRONAUTICS

at the

MASSACHUSETTS INSTITUTE OF TECHNOLOGY

JANUARY 2000
[February 2000]

Author: _____
Department of Aeronautics and Astronautics
January 17, 2000

Certified by: _____
Professor Alan H. Epstein
R. C. Maclaurin Professor of Aeronautics and Astronautics
Thesis Supervisor

Accepted by: _____
Professor Nesbitt W. Hagood
Associate Professor of Aeronautics and Astronautics
Chairman, Departmental Graduate Committee

SYSTEMS ANALYSIS OF A MICROFABRICATED STORABLE BIPROPELLANT ROCKET ENGINE

by

CHRISTOPHER S. PROTZ

Submitted to the Department of Aeronautics and Astronautics
on January 17, 2000 in Partial Fulfillment of the
Requirements for the Degree of Master of Science in
Aeronautics and Astronautics

ABSTRACT

This thesis discusses the systems analysis of a storable bipropellant micro-rocket engine. Micro-rockets are built using MEMS technology and are projected to deliver a thrust to weight ratio up to two orders of magnitude greater than conventional rocket motors at small thrust levels making them very attractive for satellite propulsion applications and propulsion of very small launch vehicles.

Several propellant combinations and engine cycles have been analyzed. Propellant combinations have been evaluated for a 125 atm combustion chamber on the basis of their performance, handling, and cooling properties. A non-toxic hydrogen peroxide/ethanol combination (302 s Isp) is chosen over a nitrogen tetroxide/hydrazine combination (322 s Isp) and a hydrogen peroxode/JP-7 combination (315 s Isp) on the basis of handling and cooling properties. Studies indicate that nitrogen tetroxide/hydrazine expander and decomposition topping cycles and hydrogen peroxide/ethanol and hydrogen peroxide/JP-7 decomposition topping cycles are feasible. It is shown that a 300 atm turbopump feed system is possible while further investigations on bearings and pump design are required to fully validate the concept.

The analysis suggests that the storable bipropellant micro-rocket engine concept is feasible and identifies the engineering challenges ahead.

Thesis Supervisor: Professor Alan H. Epstein
Title: R. C. Maclaurin Professor of Aeronautics and Astronautics

ACKNOWLEDGMENTS

I would like to thank my parents for giving me the opportunity to attend MIT in the first place and for giving me their constant support throughout my education.

I would like to thank my advisor, Prof. A. H. Epstein for the opportunity to work on this project. His guidance throughout the project was invaluable. Prof. J. L. Kerrebrock's discussions and guidance were also very helpful.

Prof. M. Martinez-Sanchez, Col. Pete Young, and Dr. Gerald Guenette also gave me valuable advice throughout the course of this project.

Adam London helped me to come up to speed with the micro-rocket project and continued to help by answering my frequent questions. I have also enjoyed working with the micro-rocket researchers, Adriane Faust, Rick Francis, and Antoine Deux.

I wish to thank my friends at the GTL for helping to make daily life that much more enjoyable. Thank you to my brother, Jon Protz, Nick Savoulides, Dan Kirk, Bruno Miller, Tony Chobot, Kevin Lohner, Chris Spadaccini, Waleed Farahat, and Mez Polad.

This work was supported by an NDSEG Fellowship from the US Army. This support is gratefully acknowledged.

TABLE OF CONTENTS

LIST OF FIGURES

LIST OF TABLES

CHAPTER 1

INTRODUCTION

1.1 Background and Motivation

1.1.1 Concept

Micro-rocket engines, under development at MIT, are highly compact rocket engines that are projected to deliver a thrust to weight ratio that is up to 100 times that of current rocket engines. At present, small thrusters exist that use pressurized tanks to drive the propellants into the chamber. These thrusters typically rely on radiation for cooling. Micro-rocket engines will have an integrated pumping system and regenerative cooling system. This pumping system eliminates the need for pressurized tanks, thus reducing the structural tank mass. The regenerative cooling system expands the applications of the engine by allowing prolonged operation.

The idea of micro-rocket engines for orbit maintenance and control was presented by London [London, 1996]. These engines derive their high thrust to weight ratio from the fact that as the size is decreased the thrust of the engine only falls with the area of the nozzle exit, or a characteristic length squared, while the mass of the engine falls with the cube of the characteristic length. The engine thrust is

$$T \propto P_c A_t C_F \tag{1-1}$$

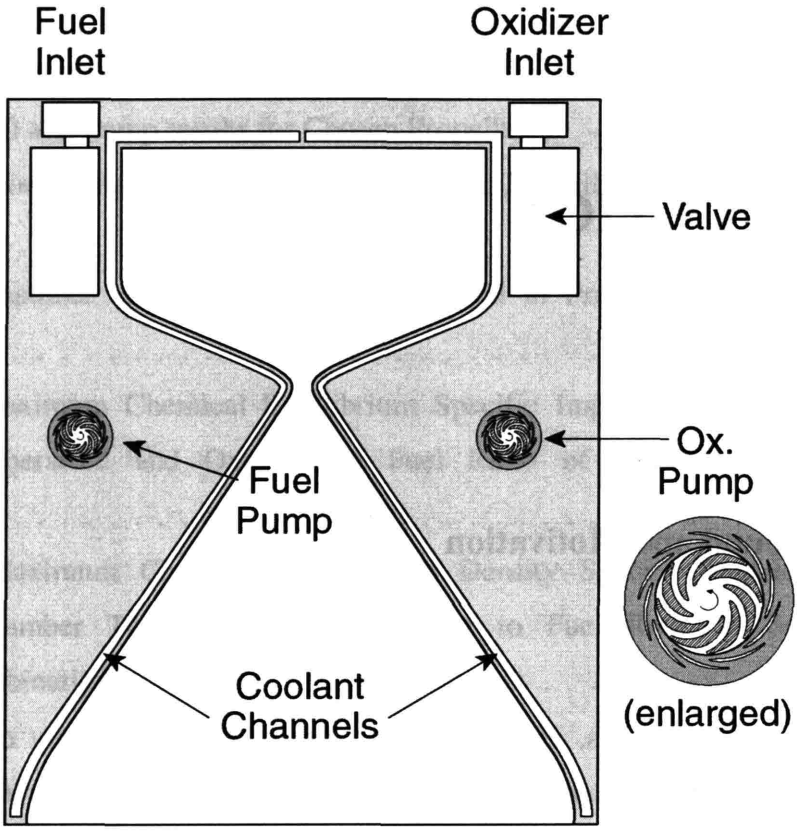

Figure 1-1: Preliminary System Layout of Micro-Rocket Engine (not to scale) [Courtesy Adam London, 1999].

and the engine weight can be written

$$W \propto \rho g L \varepsilon A_t \tag{1-2}$$

P_c is the chamber pressure, A_t the throat area, C_F the thrust coefficient, ε the nozzle expansion ratio, L the engine length, ρ the density of silicon, and g the acceleration of gravity. Approximating ε ~ 10, $P_c \sim 10^7$ Pa, $L \sim 10^{-2}$ m, $C_F \sim 1$ and $\rho \sim 1000$ kg/m^3 then

$$\frac{T}{W} \cong \frac{10^7}{(10^3)(10)(10^{-2})(10)} \cong 10^4 \tag{1-3}$$

This is 100 times that of traditional chemical liquid bipropellant engines [Al-Midani].

The micro-rocket engine system employs a regeneratively cooled combustion system, in which the propellants are used to cool the structure before entering the combustion chamber. A turbopump feed system is employed to pressurize the propellants. The pumps are driven by turbines, which are driven by the expansion of hot gasses. A control system is used for safety and to maintain engine operation. The success of the micro-rocket engine depends on the ability to manufacture micro-turbopumps to pressurize the propellants and a cooling scheme to sufficiently cool the surface area of the main combustion chamber, which has a larger surface to volume ratio than larger engines. A regeneratively cooled combustion chamber with cooling passages is currently being fabricated and tested [London, 1999]. The propellants are supplied from an externally pressurized source. Detailed design and test of a turbopump feed system will be carried out in the future.

1.1.2 Manufacturing Micro-Rockets

Individual micro-rocket engine wafers are to be constructed using microelectrical and mechanical systems (MEMS) technology through methods similar to those used to construct integrated circuits. MEMS is a technology has the potential to revolutionize power and energy production in the same way the silicon chip did for computing power. By employing the technological and industrial base of the microprocessor industry, MEMS researchers aim to create miniaturized actuators, sensors, power generators, and even propulsion sources with a characteristic length of centimeters at very low cost.

A single engine will be made of a stack of several silicon wafers. Each wafer undergoes an intricate etching process that creates complex features in the depth of the wafer. This process, microfabrication, allows only planar features to be formed in the depth of each wafer. To build complex three-dimensional structures, such as micro-turbopumps using this technique, several wafers must be processed individually and bonded [Al-Midani]. The present design of the engine consists of six wafers bonded together [London, 1999]. Different wafers will hold features of the pump inlet and blades, the turbine inlet and blades, the journal bearing between the pump and turbine,

and the cooling passages. Figure 1-2 shows a schematic of the six wafers of the pressure fed micro-rocket. One layer of this device is shown in Figure 1-3.

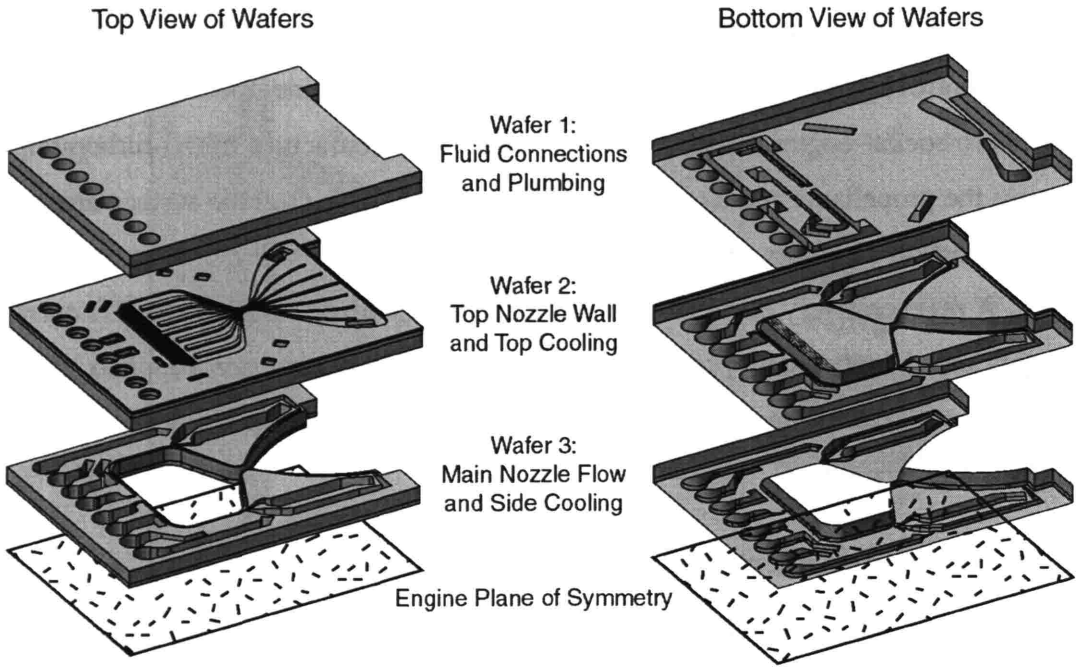

Figure 1-2: Micro-Rocket Engine Wafer Layout and Assembly [Courtesy Adam London, 1999].

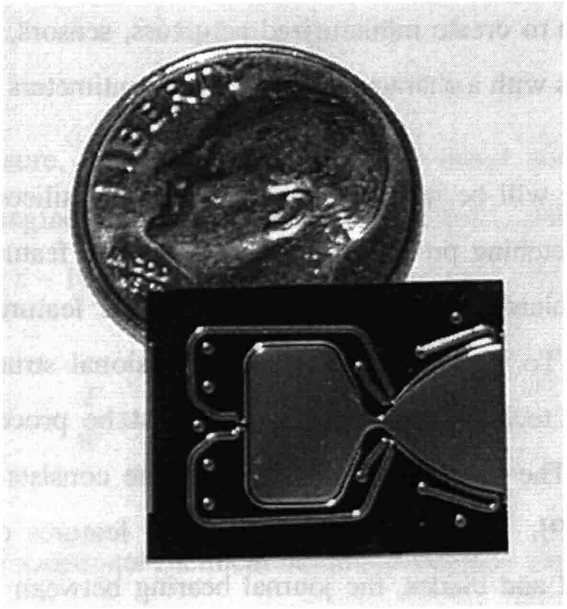

Figure 1-3: Micro-Rocket Engine Chip (1 Layer) [Courtesy Adam London, 1999].

1.1.3 Advantages

Micro-rocket engines offer a much greater thrust-to-weight ratio than present rocket engines, as shown briefly above. This improvement leads to a decrease in overall launch system weight. This means more payload can be delivered at the same cost of propellants and overall mass. Another important advantage is that, if many small engines are used on a single vehicle, a single failure of one small micro-engine is much less likely to result in a complete loss of the vehicle and payload. Micro-rocket engines could be used redundantly because of their low engine weight. Large engine failures often result in explosions that destroy the entire vehicle, or the vehicle has to be manually destroyed if the failure results in a loss of control of the vehicle. Control may be able to be maintained even with a failure.

Another advantage results from the fabrication method. Since the cost of production is not directly linked to the complexity of features of the unit, very complex designs can be produced without a corresponding increase in cost.

The small size and thrust level of the rocket engine and the fact that many engines may be used on one stage of a vehicle means that one size of the engine can be used for all applications. Any desired thrust level (in multiples of one engine's thrust) can be achieved simply be stacking several engines. Since thrust depends primarily on nozzle exit area given a fixed expansion ratio, ε, and chamber pressure, P_C, the significant weight savings of the micro-rocket engine can be taken advantage of on nearly any size vehicle. This is the basis of the micro-launch vehicle discussed in the next section.

1.1.4 Applications

It has been shown that micro-bipropellant rockets would be useful for orbital maneuvers such as orbital insertion or rephasing. It has also been shown that significant weight savings of the system would allow them to be useful as propulsion for transfer stages of geosynchronous satellites, where their transfer times would be significantly less

than those envisioned for electric propulsion [London, 1996]. An effort is currently ongoing to explore the possibility of using micro-rocket engines as the only source of propulsion on a very small launch vehicle. This air-launched vehicle would deliver 1 kg to geosychronous orbit with a 78 kg gross liftoff weight launch vehicle [Francis].

1.2 Objectives

An analysis was performed that showed that the micro-rocket engine cycle was feasible with liquid oxygen as the oxidizer and ethanol as the fuel, except for one seemingly insurmountable difficulty. There seems to be no simple way to avoid vaporization of the LOX at the inlet to the turbopump, which must be integrated to a nearby isothermal engine assembly [Al-Midani]. Accordingly, it has been determined that the micro-rocket must use storable propellants, which in addition to solving this problem can be handled and stored at ambient conditions, as opposed to cryogenic fuels, which must be stored at low temperatures. Additionally, storable propellants ease operations such as transporting the engine and fueling the tanks and can be stored for extended periods of time in the tanks until the engine is needed.

The focus of this effort is to evaluate possible storable propellant combinations, engine cycles, and engine components of a turbopump fed, storable liquid bipropellant, microfabricated, rocket engine.

1.3 Project Challenges and Thesis Overview

Turbomachinery

Aspects of the turbopump system and its components are discussed in chapters 3 and 4, but no detailed design has been developed. Design of this system is scheduled to be performed in the near future. This will include design of the pumps, turbines, and bearings.

Propellant Combination

The choice of fuel and oxidizer is varied. The propellants are compared based on their compatibility with other materials, their storage and handling requirements, their ignition characteristics, their cooling properties, and their performance. Several propellant combinations are considered to show how performance and complexity of the system change with different combinations. Propellants are discussed in Chapter 2.

Engine Cycle

The choice of engine cycle is varied. Engine cycles differ in how they provide heat to the turbine drive gas and in how they provide coolant to the chamber and nozzle. Several candidate cycles are considered, and their effects on performance and complexity of the system are noted. Two cycles, the decomposition topping cycle, and the expander cycle are analyzed in further detail. This is discussed in Chapter 3.

Valves and Control

Micro-rocket engines do not require the same high pressure valves that are used in small pressure-fed thrusters. Micro-rocket engines do require low pressure valves at the tank exit to deliver the propellants to the pumping system. These valves should weigh much less than current high pressure valves. Micro-valve design has not yet been pursued for rocket applications.

Combustion, Injection, and Mixing

These aspects of the engine were examined previously [Al-Midani], and a pressure-fed micro-rocket engine will soon be tested to determine if mixing on these scales can be achieved with the present design [London, 1999].

Cooling

Cooling the micro-rocket engine is necessary because the chamber temperature is 1500 K above the melting point of silicon. A cooling system design must ensure that the wall temperatures remain at an acceptable level. The cycle design must ensure that there is enough heat capacity in the coolant (propellants) to achieve this goal. Cooling system

design has been studied as part of another research effort, and is soon to be validated [London, 1999].

Packaging and Propulsion Integration

The micro-rocket engine must be connected to macro devices such as tanks, testing apparatus, and instrumentation. Fittings between the silicon structure of the engine and non-silicon components outside of the engine are necessary. This task has been studied as part of a separate research effort [London, 1999].

Construction

The micro-rocket engine will be constructed from six silicon wafers. Features must be created in each wafer, and these wafers must be aligned and bonded to each other to create the whole structure. Experiments have shown that these structures can be made [London, 1999].

CHAPTER 2

PROPELLANT ANALYSIS

The first step in the evaluation of the system is to analyze the suitability and performance of possible propellant combinations for the system. A summary of the handling, storage, and materials compatibility data is presented. The performance of several candidate propellant combinations is evaluated, and two combinations are selected. Finally, the cooling ability of each propellant combination is discussed.

First candidate propellants must be chosen. A list of possibilities is shown in Table 2-1.

Table 2-1: List of Possible Propellants.

Oxidizers	Fuels
Cryogenic	
Oxygen (O_2)	Hydrogen (H_2)
Flourine (F_2)	Methane (CH_4)
Non-Cryogenic	
Nitrogen Tetroxide (N_2O_4)	Pentaborane (B_5H_9)
Red Fuming Nitric Acid (NO_2)	Ethyl Alcohol (Ethanol) (C_2H_6O)
Hydrogen Peroxide (H_2O_2)	Hydrazine (N_2H_4)
	UDMH [$(CH_3)_2NNH_2$]
	Aerozine 50 (50% N_2H_4 / 50% UDMH)
	MMH (CH_3NHNH_2)
	Hydrocarbons (CH_n)

This is by no means an exhaustive list of possible rocket propellants, but it includes several of the most popular propellant choices, and some of the ones with the highest performance. From this list, the cryogenics are removed because the design is required to use storable propellants.

From the oxidizers, red fuming nitric acid is removed because, while it offers slightly better performance with most fuels, it is not used extensively today in the United States, so it is not readily available. Nitrogen tetroxide is available and offers similar performance.

From the fuels, pentaborane is eliminated from this study because, while it offers superior performance, it is extremely toxic and corrosive. Further, it is not readily available, because it is not used in many applications today.

A list of the storable propellant options considered in more detail is shown in Table 2-1. UDMH is unsymmetrical dimethylhydrazine, and aerozine 50 is a mixture of 50% hydrazine and 50% UDMH.

Table 2-2: List of Propellants Examined in More Detail.

Oxidizers	Fuels
Nitrogen Tetroxide	Ethyl Alcohol (Ethanol)
Hydrogen Peroxide	Hydrazine
	UDMH
	Aerozine 50
	MMH
	Hydrocarbons

These propellants are among the highest performing storable propellants if fuels containing beryllium are not considered [Sutton]. Nitrogen Tetroxide is the most commonly used storable oxidizer [Sutton]. It is often used with hydrazine and hydrazine derivative fuels. Hydrogen peroxide is a relatively safe and available oxidizer. The hydrocarbon fuels that are considered are JP-5 and JP-7. They are similar propellants, but JP-7 forms less carbonaceous deposits than JP-5 [Kerrebrock, 1999]. These deposits could clog cooling passages. Performance and cooling results are calculated for JP-5 because data was not available on JP-7.

2.1 Propellant Properties, Compatibility, Storage, and Handling

2.1.1 Fuels

2.1.1.1 Hydrazine

Hydrazine (N_2H_4) is a clear liquid with a density of 1023 kg/m^3. Its normal boiling point is 386.7 K and its normal freezing point is 274.3 K. Often unsymmetrical dimethylhydrazine (UDMH) $(CH_3)_2NNH_2$ or monomethylhydrazine (MMH) (CH_3NHNH_2) are added to hydrazine. They stabilize hydrazine at higher temperatures and reduce the freezing temperature, but these additives do lower the specific impulse of hydrazine propellant combinations [Primex, Schmidt, Sutton].

Hydrazine vapor is irritating to the eyes, mucous membranes, and skin. Hydrazine splashes that contact the skin or eyes can cause severe burns or permanent damage. Toxic amounts of hydrazine can be taken into the body by inhalation or absorption through the skin [Pillori]. Safety goggles and a face shield, a protective suit, proper gloves, and a chemical cartridge respirator with organic vapor cartridge are recommended for handling hydrazine,

Pure hydrazine can be stored in sealed tanks for over 15 years and safely heated above 530 K. Contaminated hydrazine will decompose violently at 367 K. Materials compatible with hydrazine include 303, 304, 321, and 347 stainless steel, nickel, tantalum, and 1100 and 3003 aluminum. Iron, copper, and its alloys (brass and bronze), monel, magnesium, zinc, and other aluminum alloys must be avoided [Pillori, Schmidt, Sutton].

Hydrazine can be used as an etchant for silicon microfabrication. The etch rate of silicon in hydrazine is between 10 μm to 100 μm per hour [Mehregany and Senturia]. This etch rate is unacceptable. The structure of the engine cannot be allowed to be etched away by the propellant. Fortunately, silicon can be protected from hydrazine with thin film coatings. The masking material would not be etched at a significant rate by the

hydrazine, and it would prevent the hydrazine from contacting the silicon. "Silicon dioxide and silicon nitride are etched very slowly, providing excellent masking ability. The etch rate of silicon dioxide (thermally grown at 990 C and 95 C steam) was measured to be close to 100 Å/h at 118 C. The etch rate of Si_3N_4 is smaller but could not be measured accurately" [Mehregany and Senturia]. Highly boron-doped silicon is not etched in hydrazine. Silver, Gold, Titanium, and Tantalum sputtered films are not etched by hydrazine either [Mehregany and Senturia].

2.1.1.2 Ethanol

Ethanol is a clear liquid with a density of 780 kg/m^3. Its normal boiling temperature is 351.5 K, and its normal freezing temperature is 159 K [Kakac].

Ethanol can be stored indefinitely and does not have the serious handling limitations of the propellants listed above. Its ability to act as a coolant in the micro-rocket has recently been demonstrated [London, 1999].

2.1.1.3 JP-7

JP-7 is a liquid hydrocarbon fuel projected for use in turbojets, where its endothermicity enables effective fuel-cooling of bearings and other parts. It is favorable as a rocket propellant because it does not coke, form solid carbonaceous deposits, as much as other hydrocarbon fuels at high temperatures [Kerrebrock, 1999]. This is important in the cooling passages of the micro-rocket, however, its anti-coking properties at the heat fluxes required by the micro-rocket (~100 W/mm^2) are not certain [Edwards]. JP-7 can be stored for extended periods of time and does not have serious handling limitations.

2.1.2 Oxidizers

2.1.2.1 Nitrogen Tetroxide

Nitrogen tetroxide (N_2O_4) is a heavy (density of 1440 kg/m^3) reddish-brown liquid with a normal boiling point of 294.35 K and a normal melting point of 261.95 K [USAF].

Nitrogen Tetroxide is insensitive to all types of mechanical shock and impact [USAF]. It is mildly corrosive when pure, but forms strong acids when combined with moisture. It has a high vapor pressure (1.18 atm) and its vapor combines with moisture in the air. For this reason, it is highly corrosive to the eyes, skin, and the pulmonary tract. Protective clothing for proper handling includes a full-face respirator, acid resistant clothing and gloves, and a full face shield [Green].

Nitrogen tetroxide can be stored indefinitely in sealed containers made of compatible material. Some compatible materials are Titanium, 321 Stainless Steel, Tantalum, tungsten, 3003 and 5052 Aluminum, anodized aluminum. Materials not compatible for storage but compatible for short exposure times include Inconel, platinum, and tin [USAF]. Materials that must be avoided include most other metals, water, bases and organic material [Green, USAF].

Nitrogen tetroxide is a strong oxidizer. In contact with silicon, it reacts with the surface and causes a thin layer of SiO_2 to grow. This layer serves as a strong diffusion barrier to the oxygen and prevents more SiO_2 from being formed [Senturia]. Therefore, nitrogen tetroxide and silicon are compatible at room temperature. Testing will be necessary to determine if nitrogen tetroxide and silicon are compatible at high temperatures.

2.1.2.2 Hydrogen Peroxide

Hydrogen peroxide is a heavy (density of 1443 kg/m^3) clear liquid with a normal boiling point of 422 K and a normal freezing point of 273 K [FMC]. Hydrogen peroxide is used in concentrations between 70% and 98% in rocket applications, with the rest being water [McCormick].

Short-term exposure to concentrated hydrogen peroxide and its vapors causes temporary irritation of the skin and eyes. Prolonged exposure can have more severe and permanent effects. Safety goggles and plastic or rubber shoes are required when handling concentrated hydrogen peroxide. Clothing must be made of Dacron, Dynel, or Orlon, as ordinary fabrics are apt to ignite when splashed with hydrogen peroxide [McCormick].

Pure concentrated hydrogen peroxide is generally more stable than dilute solutions [Shell]. Materials suitable for storage include Pyrex glass, 1060 and 1260 aluminum, tantalum, and zirconium. Ninety percent hydrogen peroxide has been stored for up to 3 years. Storage tests with ninety-eight percent hydrogen peroxide indicate storage through a five year period is feasible [McCormick]. Care must be taken to ensure that the hydrogen peroxide does not become contaminated. Properly stored hydrogen peroxide typically decomposes at a rate of 1% per year. The tank must permit the decomposition products to escape, and the tank must be monitored for an increase in temperature. If a tank experiences a temperature increase due to decomposition of the hydrogen peroxide, the contents must be disposed of immediately, because the decomposition rate increases sharply with temperature [McCormick].

Hydrogen peroxide is a strong oxidizer and combines with silicon to form a thin layer of SiO_2, much like Nitrogen Tetroxide. Hydrogen peroxide is compatible with silicon under standard conditions as evidenced by its use in microfabrication cleaning steps. Short term contact of hydrogen peroxide with silicon is permitted, but should not exceed 4 hours at 344 K or 1 week at 294 K [Pillori]. High temperature oxygen and steam (which are also the decomposition products of hydrogen peroxide) are used to grow oxide layers, however. Testing will be necessary to determine if hydrogen peroxide and silicon are compatible at high temperatures.

2.1.3 Summary of Propellant Properties

The following table lists the relevant properties of the propellants listed above. ρ is the density, Pc and Tc are the critical pressure and temperature, respectively, Tb is

the normal boiling point, Cp is the specific heat at 1 atm and 300 K, and VP is the vapor pressure at 300K.

Table 2-3: Properties of Propellants Considered [Primex, FMC, Pillori, USAF, Kakac, Barin].

	Chemical Formula	ρ [kg/L]	Pc [atm]	Tc [K]	Tb [K]	Cp [J/kg/K]	VP at 300 K [atm]
Fuels							
Hydrazine	N_2H_4	1.023	145	653.1	386.7	3690	0.0189
Ethanol	C_2H_6O	0.780	62.8	515.8	351.5	2456	0.0775
JP-7		0.800				2093	0.136
Oxidizers							
Nitrogen Tetroxide	N_2O_4	1.440	100	431.4	294.4	3087	1.18
Hydrogen Peroxide	H_2O_2	1.443	214	730	422	2590	0.00658

2.2 Propellant Performance

The propellant combination performance is determined through the use of the Computer Program for Calculation of Complex Chemical Equilibrium Compositions and Applications, CEA. CEA determines the chemical equilibrium point of the mixtures by minimizing the Gibbs energy and determines the theoretical rocket performance using one-dimensional equations [Gordon and McBride]. Chemically frozen flow is assumed during expansion through the nozzle. The parameters chosen are as follows:

Table 2-4: Chamber and Nozzle Parameters Used in Propellant Performance Analysis.

Chamber Pressure	125 atm
Chamber Area: Throat Area	16:1
Nozzle Area: Throat Area	15:1
Back Pressure	Vacuum
Oxidizer Inlet Temperature	298.15 K
Fuel Inlet Temperature	298.15 K

Assuming the above parameters CEA can be used to determine the specific impulse and chamber temperature of the propellant combinations. Equation 2.1 is used to determine the density specific impulse of the propellants. It is the specific impulse weighted by the density of the propellants. The higher the density of the propellants, the less tank volume is needed for a given mass of propellants. This results in less structural mass of the vehicle, and less aerodynamic drag. Therefore, high density specific impulse is desired.

$$\begin{cases} I_d = \rho_{av} I_{sp} \\ \rho_{av} = \dfrac{\rho_o \rho_f (1+r)}{r(\rho_f) + \rho_o} \end{cases} \tag{2.1}$$

where I_d is the density specific impulse of the combination, ρ_{av} is the average density of the mixture, I_{sp} is the specific impulse of the combination, ρ_o is the oxidizer density, ρ_f is the fuel density, and r is the oxidizer to fuel mass ratio.

The results are shown below in Table 2-5. The hydrazine/nitrogen tetroxide system has the highest specific impulse capability (322 s), and the JP-5/hydrogen peroxide system has the highest density specific impulse because the oxidizer to fuel ratio is very large (7.0), and the oxidizer has a relatively high density (1443 kg/m^3). These combinations are selected for further analysis based on their performance and on their properties as discussed above and in Chapter 3. The ethanol cycles have the worst performance by both measures. Figures 2-1 and 2-2 show Isp and Id vs. oxidizer to fuel ratio.

Table 2-5: Maximum Specific Impulse, Associated Chamber Temperature, and Oxidizer to Fuel Ratio of Selected Propellant Combinations Assuming Flow Chemically Frozen From the Throat to the Nozzle Exit.

	O/F Ratio	Chamber Temperature	Isp [s]	Id [g*s/m^3]
Hydrazine/N_2O_4	1.2	3256	322	375
Hydrazine/H_2O_2	1.8	2915	318	379
JP-5/N_2O_4	3.4	3603	313	371
JP-5/H_2O_2	5.8	3118	315	386
Ethanol/N_2O_4	2.4	3250	296	326
Ethanol/H_2O_2	4.0	2904	302	351

Table 2-6: Maximum Density Specific Impulse, Associated Chamber Temperature, and Oxidizer to Fuel Ratio of Selected Propellant Combinations Assuming Flow Chemically Frozen From the Throat to the Nozzle Exit.

	O/F Ratio	Chamber Temperature [K]	Isp [s]	Id [g*s/m^3]
Hydrazine/N_2O_4	1.3	3301	308	394
Hydrazine/H_2O_2	2.0	2946	302	403
JP-5/N_2O_4	3.8	3660	301	388
JP-5/H_2O_2	6.6	3130	298	410
Ethanol/N_2O_4	3.0	3310	281	347
Ethanol/H_2O_2	4.4	2905	286	374

Figures 2-3 and 2-4 show I_{sp} and I_d vs. chamber temperature. If the chamber temperature is limited by material constraints these two plots tell what specific impulse and density specific impulse would be expected at that chamber temperature. The hydrazine/nitrogen tetroxide and hydrazine/hydrogen peroxide combinations offer the best performance for any given chamber temperature. The hydrazine/nitrogen tetroxide combination has a higher peak temperature and I_{sp} as show above. The JP-5/hydrogen peroxide combination has the next best I_{sp} up to 3100 K.

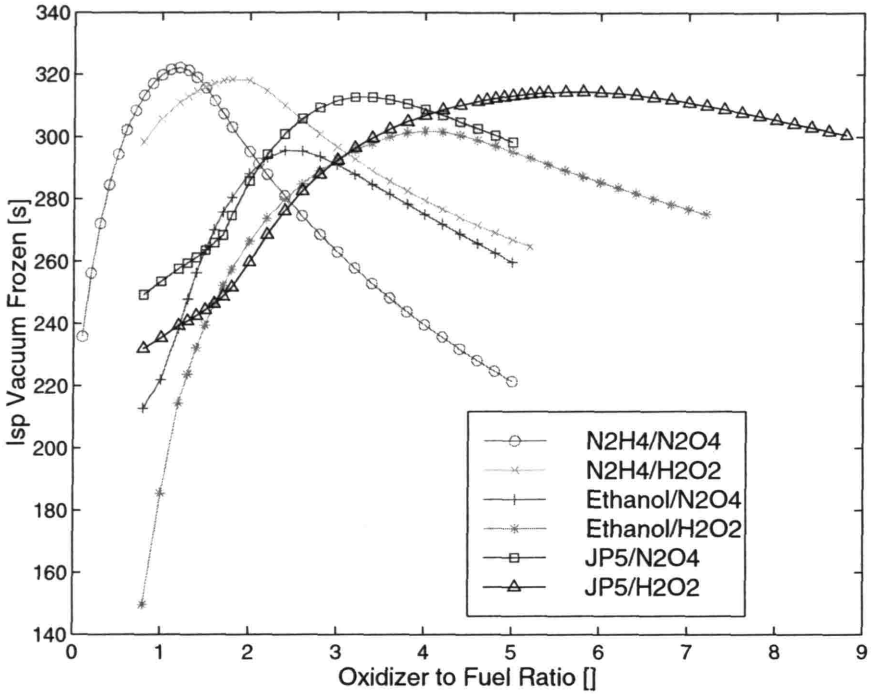

Figure 2-1: Vacuum Specific Impulse vs. Oxidizer to Fuel Ratio of Selected Propellant Combinations Assuming Flow Chemically Frozen from the Throat to the Nozzle Exit.

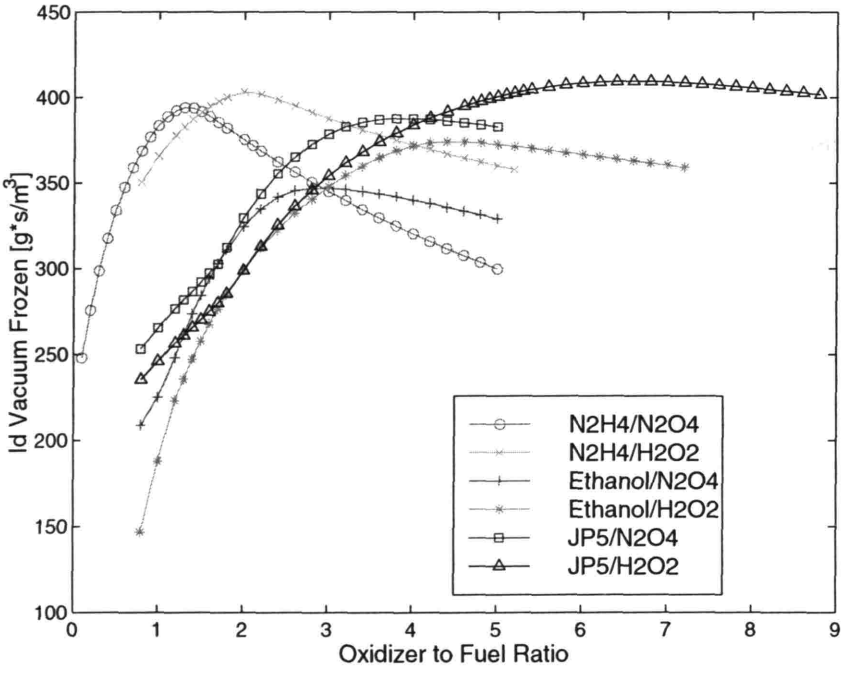

Figure 2-2: Vacuum Density Specific Impulse vs. Oxidizer to Fuel Ratio of Selected Propellant Combinations Assuming Flow Chemically Frozen from the Throat to the Nozzle Exit.

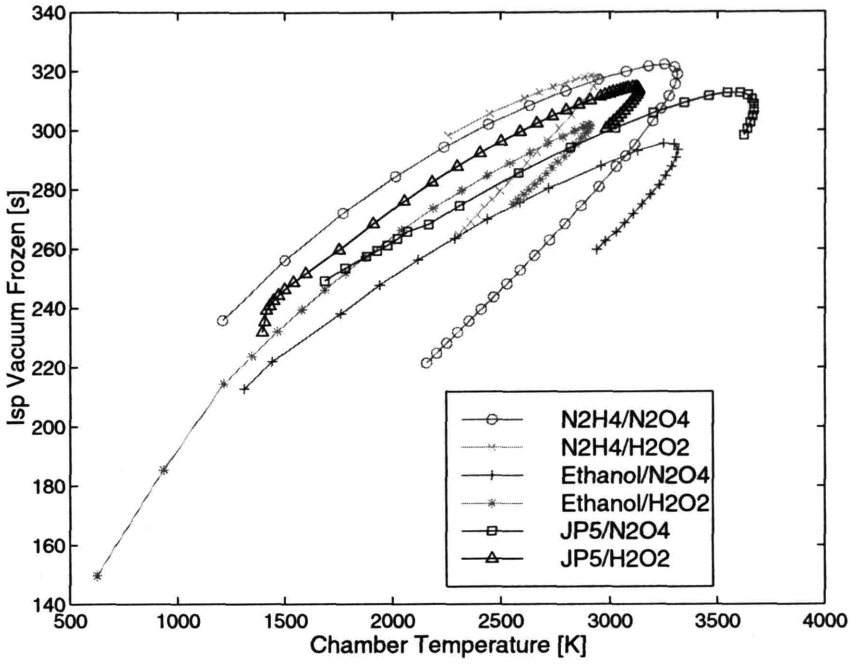

Figure 2-3: Vacuum Specific Impulse vs. Chamber Temperature of Selected Propellant Combinations Assuming Flow Chemically Frozen from the Throat to the Nozzle Exit.

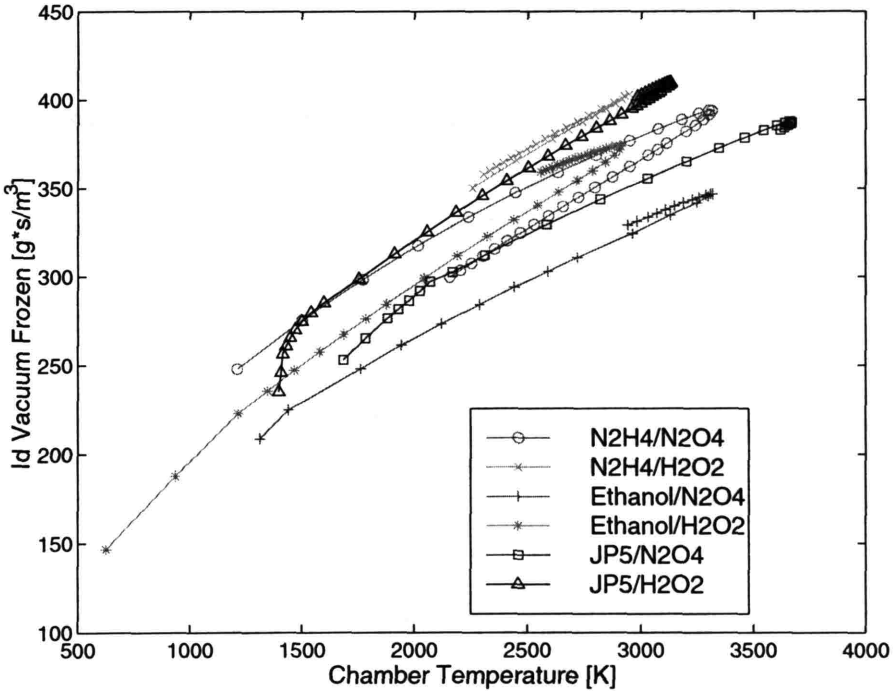

Figure 2-4: Vacuum Density Specific Impulse vs. Chamber Temperature of Selected Propellant Combinations Assuming Flow Chemically Frozen from the Throat to the Nozzle Exit.

2.3 Propellant Coolant Analysis

The cooling requirements for the chamber and nozzle of the hydrogen peroxide/JP-7, hydrogen peroxide/ethanol, and hydrazine/nitrogen tetroxide system are analyzed and discussed below. The cooling capacity of the micro-rocket engine system is then evaluated with respect to the size of the engine.

The fundamental limit on the cooling capacity of the rocket engine system is based on the total heat capacity of the propellants used as coolant. In steady-state operations, all the heat must be absorbed in the coolant. During transients, the bulk silicon of the structure may be able to be used as a heat sink. If heat were absorbed by the bulk in steady state operations the structure would overheat rapidly. A thermal balance is performed based on the heat capacity and mass flow rates of the coolants and the maximum wall temperature. The chamber and nozzle geometry of the thrust chambers being tested is shown in Figure 2-5.

CEA is used to find the fluid properties at the throat. For the geometry above this results in the following mass flow rates for each propellant combination. These flow rates are necessary for the analysis below in section 2.3 in order to determine the temperature rise of each propellant used as a coolant.

Table 2-7: Mass Flow Rates for Different Propellant Combinations Given Micro-rocket Geometry at 125 atm Chamber Pressure and 298.15 K Initial Propellant Temperature at Specified Oxidizer to Fuel Ratio.

Propellant Combination	Oxidizer to Fuel Ratio	$\dot{m}$ [g/s]
Hydrazine/N_2O_4	1.2	5.28
Hydrazine/H_2O_2	1.8	5.39
JP-5/N_2O_4	3.4	5.43
JP-5/H_2O_2	5.8	5.21
Ethanol/N_2O_4	4.0	5.80
Ethanol/H_2O_2	2.4	5.75

For the chamber geometry below, the heat that must be removed is calculated. A wall temperature of 900K is assumed for this calculation. The local heat flux to the wall can be written

$$q = h_g (T_{aw} - T_{wg}) \tag{2.2}$$

An accurate value of the film cooling coefficient, h_g, can only be obtained experimentally. Several correlations to approximate the experimental data exist for estimating it, though. Two are employed in this analysis. Bartz's correlation is

$$h_g = \frac{0.026}{D^{0.2}} \left(\frac{C_p \mu^{0.2}}{\mathrm{Pr}^{0.6}} \right) (\rho v)^{0.8} \left(\frac{\rho_{am}}{\rho'} \right) \left(\frac{\mu am}{\mu_0} \right)^{0.2} \tag{2.3}$$

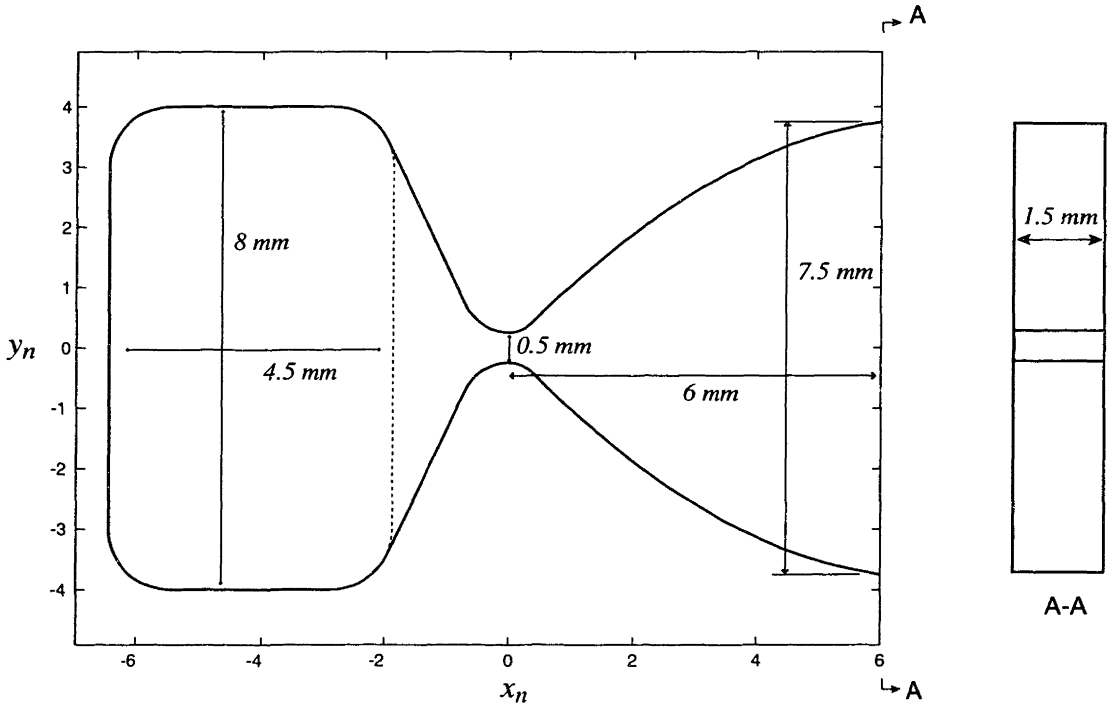

Figure 2-5: Geometry used in Chamber and Nozzle Cooling Analysis [Courtesy Adam London, 1999].

using D, the hydraulic diameter of the passage, as the critical length [Sutton]. "The subscript 0 refers to properties at the stagnation or combustion temperature. The subscript, *am*, refers to properties at the arithmetic mean temperature of the local free-stream static temperature and the wall temperatures; and ρ' is the free-stream value of the local gas density [. . .]. The gas velocity, v, is the local free-stream velocity corresponding to the density ρ'" [Sutton]. Conventional heat transfer theory gives

$$h_g = 0.026 \frac{(\rho v)^{0.8}}{D^{0.2}} \mathrm{Pr}^{0.4} \frac{k}{\mu^{0.8}} \tag{2.4}$$

using D, the hydraulic diameter of the passage, as the critical length [Sutton]. These correlations are used to find the heat flux from the injectors to the nozzle exit. One more correlation is plotted. It is suggested, along with the two previous correlations, by Hill and Peterson [Hill and Peterson]. It is the same as the conventional correlation except the Reynold's number is based on the distance from the throat.

$$h_g = 0.026 \frac{(\rho v)^{0.8}}{D^{0.2}} \mathrm{Pr}^{0.4} \frac{k}{\mu^{0.8}} \tag{2.5}$$

It is not used in later calculations because it only provides information after the throat. The conventional correlation estimates of the heat transfer coefficient are made twice. The lowest line in figures 2-6, 2-7, and 2-8 shows the heat flux from equation 2-3 with the gas properties based on the film temperature, while the upper line from equation 2-3 shows the heat flux with the gas properties based on the bulk temperature. The same is true for the two lines corresponding to equation 2-4. The film temperature is estimated

$$\begin{aligned} T_{film} &= T_{wall} + 0.23 \times (T - T_{wall}) + 0.19 \times (T_{aw} - T_{wall}) \\ T_{aw} &= T + \frac{2 \times (T_c - T)}{\gamma + 1} \end{aligned} \tag{2.6}$$

This procedure assumed a constant wall temperature of 900K. A constant wall temperature is desired so that the thermal stresses in the wall will be kept to a minimum. This constant wall temperature means that the heat flux will vary throughout the chamber and the nozzle.

CEA is used to determine the fluid properties necessary for the calculations. The heat flux varies primarily with the local volumetric flow rate. Figure 2-6 shows the heat flux versus location in the chamber and nozzle for the nitrogen tetroxide/hydrazine engine. The start of the chamber is at the far left of the plot, and the nozzle exit is at the far right. The heat flux is seen to peak at the throat. Three sets of lines are shown. The upper one represents the numerical results of Bartz's correlation (Eq. 2.3), and the lower set represents those of the conventional heat transfer correlation (Eq. 2.4) with the bulk temperature line on top, and the film temperature below. The last set shows the results from equation for bulk temperature (higher curve) and film temperature (lower curve). It is observed that the results differ significantly between the two correlations. Figures 2-7 and 2-8 show the same plot for hydrogen peroxide/JP-5 and hydrogen peroxide/ethanol respectively. Similar results are observed. Methods for obtaining the necessary local heat fluxes are discussed in section 4.2.

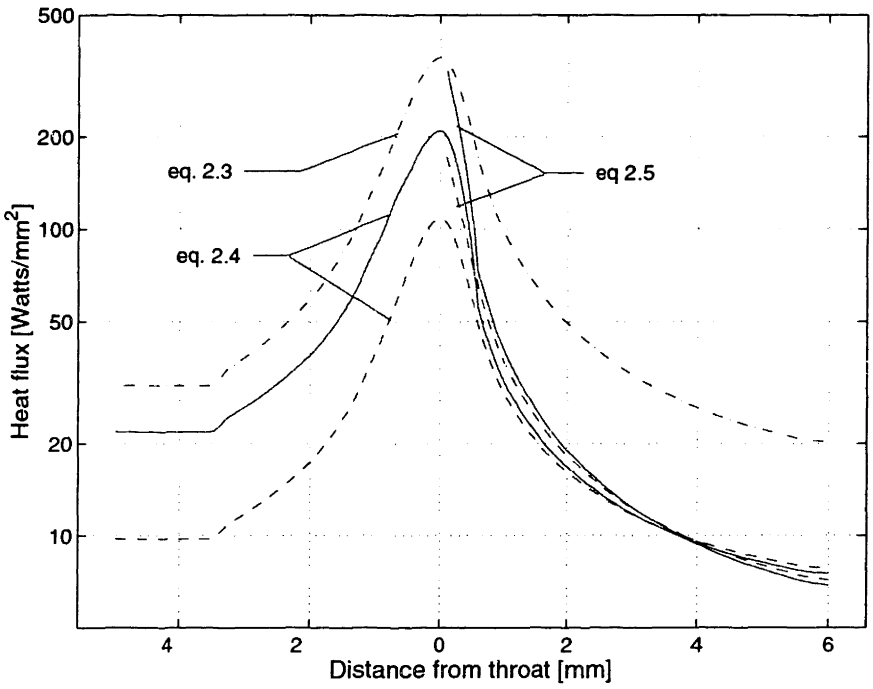

Figure 2-6: Heat Flux to the Wall Versus Distance From Throat for Hydrazine/Nitrogen Tetroxide Combination at $r = 1.2$. The Chamber is to the Left; the Nozzle is to the Right.

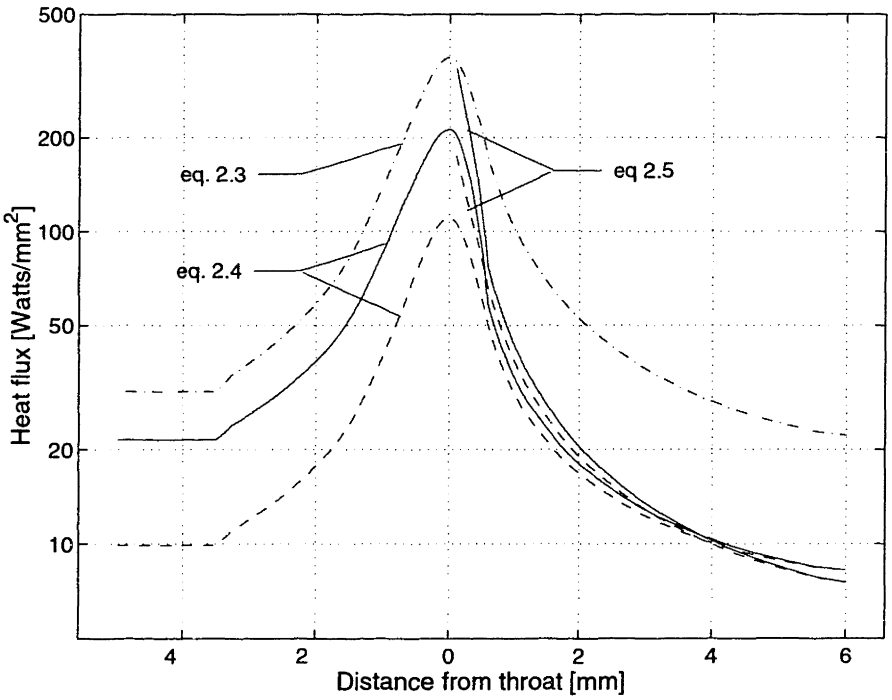

Figure 2-7: Heat Flux to the Wall Versus Distance From Throat for JP-5/Hydrogen Peroxide Combination at $r = 5.8$. The Chamber is to the Left; the Nozzle is to the Right.

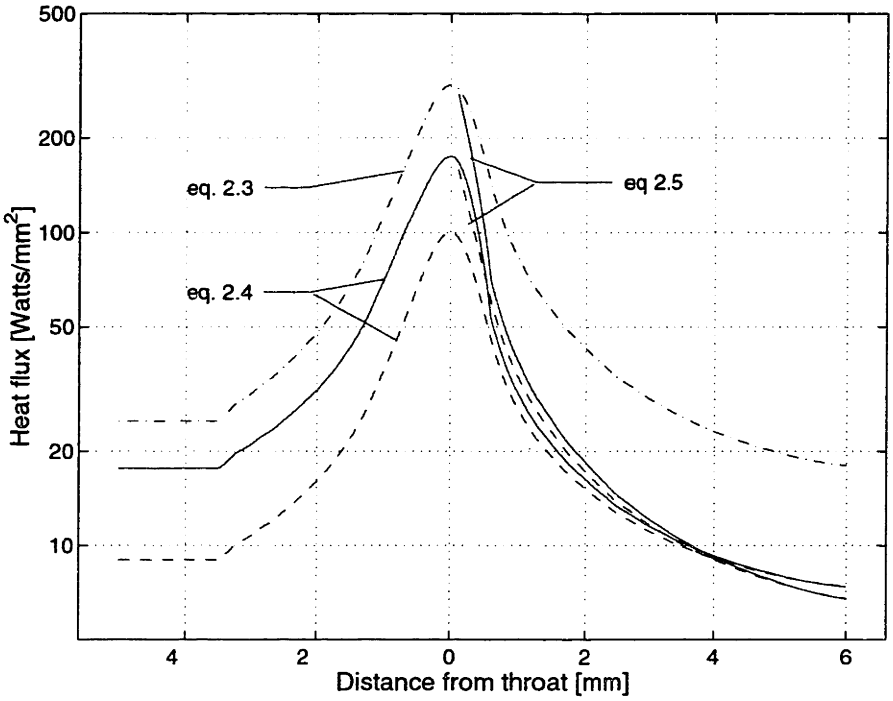

Figure 2-8: Heat Flux to the Wall Versus Distance From Throat for Ethanol/Hydrogen Peroxide Combination at $r = 4.0$. The Chamber is to the Left; the Nozzle is to the Right.

The total heat that must be absorbed by the propellants is

$$Q = \int q dA \tag{2.7}$$

This calculation is carried out based upon the previous results and the geometry of the chamber and nozzle. The heat load on the sidewalls, and at the front of the chamber is also added in the calculation. The total heat that must be absorbed by the propellant for each design is shown in Table 2-8 along with the final temperatures of the propellants based on the assumption that they absorb equal heat. This assumption is made solely to ease the calculations. Designing cooling passages so that the propellants reach the same temperature may be more desirable, but not necessarily. One propellant may cease to perform as a coolant at a lower temperature than its complement. JP-5 is used in these calculations instead of JP-7 data was not available for JP-7. The final temperatures of the

propellants shown in Table 2-8 are found by using the specific heat at one atmosphere of each of the propellants shown in table 2-3.

Table 2-8: Predicted Heat Loads and Coolant Final Temperatures for a Wall Temperature of 900 K.

		Eq 2.3		Eq. 2.4 Bulk Temp.		Eq 2.4 Film Temp.	
Propellant	Oxidizer to Fuel Ratio	Predicted Heat Load [W]	Final Propellant Temperature [K]	Predicted Heat Load [W]	Final Propellant Temperature [K]	Predicted Heat Load [W]	Final Propellant Temperature [K]
Hydrazine	1.2	8541	738	4781	545	2699	438
N_2O_4			824		593		466
Ethanol	4.0	7096	802	4043	586	2510	478
H_2O_2			777		571		469
JP-5	5.8	8710	1099	4826	743	2767	505
H_2O_2			946		657		553

The results show that the heat loads required to maintain a 900K wall temperature vary by a factor of three for a fixed propellant combination depending on the heat transfer correlation applied. The results also show that the ethanol/hydrogen peroxide requires less heat to be removed than the other cycles. This is due to the lower combustion temperature of the mixture. The hydrazine/nitrogen tetroxide and the ethanol/hydrogen peroxide mixtures have similar final propellant temperatures. This is because while the hydrazine/nitrogen tetroxide has a higher combustion temperature, its propellants also have higher specific heats. The JP-5/hydrogen peroxide cycle has a higher combustion temperature than the ethanol/hydrogen peroxide combination and lower specific heats that the other hydrazine/nitrogen tetroxide cycles. This results in higher final propellant temperatures for this combination. Data on hydrazine suggests that at 1 atm and 540K it will decompose when in contact with most materials [Pillori]. This is important because the middle estimate of the final propellant temperature the hydrazine is 545K. If it is found experimentally that more heat must be removed to maintain a 900K wall temperature, the nitrogen tetroxide would have to absorb any heat in excess of 4800W.

For the case of hydrazine and nitrogen tetroxide the estimates of the final propellant temperatures based on the specific heats at one atmosphere are compared to those based on that actual temperature-enthalpy relationship of the propellants at 250 atm (the pressure at which they enter the cooling passages). The results are shown in Table 2-9.

Table 2-9: Final Propellant Temperatures Based on Specific Heat and 300K and 1 atm and Enthalpy-Temperature Relations for Hydrazine and Nitrogen Tetroxide at an Oxidizer to Fuel Ratio of 1.2.

	Eq. 2-3 Final Propellant Temp. [K]			Eq. 2-4 Bulk Temp. Final Propellant Temp. [K]			Eq. 2-4 Film Temp. Final Propellant Temp. [K]		
Propellant	T-H Curve	Cp	T-H to Cp Difference [%]	T-H Curve	Cp	T-H to Cp Difference [%]	T-H Curve	Cp	T-H to Cp Difference [%]
Hydrazine	846	738	-12.8	654	545	-16.7	530	438	-17.4
N_2O_4	713	824	+15.6	505	593	+17.4	435	466	+7.1

These results show that all of the differences are less than 20%. This is an acceptable difference for results based on heat transfer corellations that have more uncertainty than 20%. Enthalpy-temperature relations were not found at these pressures for the other propellants.

It is not certain which heat transfer relationship or combination of relationships is the most accurate. Experimental data is necessary to determine the final propellant temperatures, however the results can be used to compare propellant combinations.

2.4 Hydrazine and Hydrogen Peroxide Decomposition Characteristics

The decomposition products of both hydrazine and hydrogen peroxide can be used to drive turbopumps. A chamber, hereafter called a decomposition chamber to avoid confusion with the main combustion chamber where the fuel and oxidizer are mixed, is used to decompose the propellant, and the resulting gases drive the turbine. It is necessary to know the temperature of these decomposition products for the design of this chamber and turbine.

For an initial temperature of 300 K the adiabatic decomposition temperature of 90% and 98% hydrogen peroxide is 1013 K and 1219 K respectively (Figure VII-8 in FMC rocket manual) and that of hydrazine ranges from 900K-1600K depending on the amount of NH_3 remaining [McCormick, Schmidt]. These decomposition temperatures vary weakly with decomposition pressure, and at 250 atm, the 90% and 98% hydrogen peroxide decomposition temperatures are 1144 K and 1283 K. These temperatures are obtained when the decomposition inlet temperature is 300 K. Research shows that the decomposition temperature also increases directly with the decomposition inlet temperature [McCormick]. The cooling system analysis above shows that the fuel in any hydrogen peroxide cycle would not have enough cooling capacity alone. This is due to the high oxidizer to fuel ratio (between 4 and 7) required for performance with these cycles. If the hydrogen peroxide reaches 700 K in the cooling passages, the decomposition temperature will be approximately 1600 K. At these temperatures the decomposition chamber would surely have to be cooled. A similar situation occurs in the hydrazine/nitrogen tetroxide decomposition cycle, but is mitigated by the fact that the optimum oxidizer to fuel ratio of the combination is 1.1 rather that 4.8 for the JP-5/hydrogen peroxide cycle. For example, if the nitrogen tetroxide is used alone as a coolant, and if the lowest estimate of heat that must be absorbed from section 2.3 is used (2700 W), the nitrogen tetroxide only reaches 624 K. If the highest estimate is used (8514 W) the nitrogen tetroxide reaches 1021 K. Again the heat flux to the wall must be determined experimentally. It determines what fraction of the heat the hydrazine has to absorb. This determines the final temperature of the hydrazine before it enters the decomposition chamber and thus the decomposition temperature. This temperature would determine if the decomposition chamber would have to be cooled for the hydrazine/nitrogen tetroxide cycle.

2.5 Propellant Conclusions

The nitrogen tetroxide/hydrazine combination provides excellent performance, but the propellants are both toxic, and it is not certain to what degree hydrazine could be used as a coolant with silicon. The hydrogen peroxide/JP-7 cycle offers non-toxic

propellants and high performance (315 s Isp), but JP-7 has not been proven as a high heat flux coolant in silicon channels. The ethanol/hydrogen peroxide combination is a favorable choice because both propellants are low toxicity propellants and require minimal special handling procedures, ethanol is a proven coolant in microdevices [London, 1999], hydrogen peroxide exhibits excellent coolant properties [McCormick], and the combination has a low chamber temperature that compensates for the relatively low specific heats of the propellants. The major drawback of this propellant choice is that its specific impulse is lower than the hydrazine/nitrogen tetroxide combination (302 s vs. 322 s frozen flow vacuum specific impulse).

CHAPTER 3

CYCLE ANALYSIS

Several candidate cycles are examined. Analysis of the decomposition and expander cycles is presented. The power requirements, assumptions, and pressure requirements of each cycle are presented, and the valid operating range of each cycle is shown graphically.

3.1 Introduction to Rocket Engine Pumping Cycles

In liquid propellant rocket engines the propellants must be forced into the combustion chamber at a pressure higher than the chamber pressure. The two general types of propellant feed systems are gas-pressure systems and turbopump propellant feed system. In a gas-pressure feed system propellants are forced out of their tanks by displacing them with high-pressure gas. A turbopump feed system uses pumps to pressurize the propellants. These pumps are driven by turbines, which are driven by the expansion of hot gasses [Sutton]. A turbopump feed system has been selected for the micro-rocket engine, as mentioned previously. Turbopump feed systems differ based in the cycle they employ, that is in how the propellant flows are routed through the system, and in where the energy necessary to drive the turbine comes from. Different cycle designs are presented and described below. Their differences, advantages, and drawbacks are detailed.

3.1.1 Decomposition Topping Cycle

The decomposition topping cycle uses decomposition product gases of either the fuel or oxidizer to drive the turbopumps, and these gases are injected into the combustion chamber after exiting the turbines. Figure 3-1 shows a schematic of this cycle.

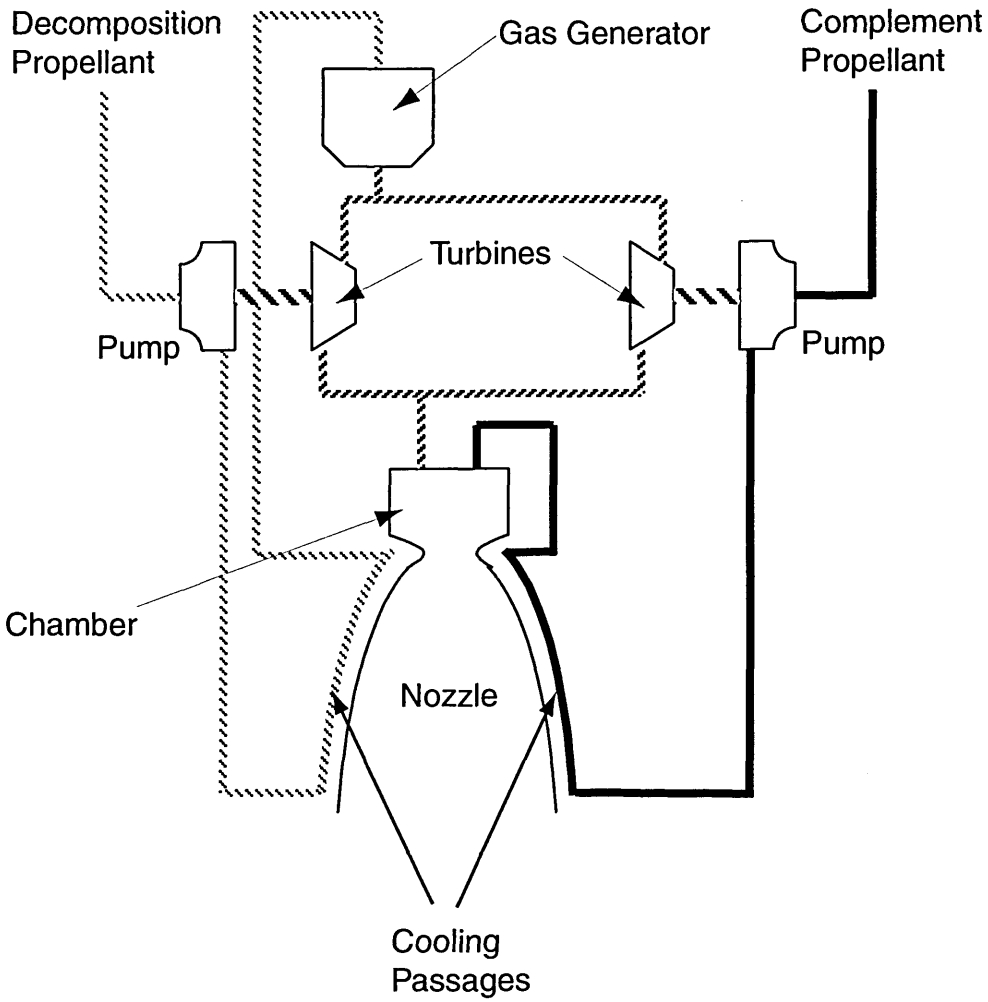

Figure 3-1: Decomposition Topping Cycle Flow Paths and Components.

Two candidate propellants are considered for decomposition, hydrogen peroxide and hydrazine. Both will have their decomposition rates accelerated by a catalyst, possibly silver, deposited on a structure designed to provide a large surface area of catalyst, a catalyst bed. Although Unsymmetrical dimethylhydrazine, UDMH, can be used as a coolant, it is not considered as it is not suitable for decomposition, since it

destroys current technology catalyst beds. Hydrogen peroxide decomposes into high temperature steam and oxygen. Hydrazine decomposes into a mixture of N_2, H_2, and NH_3. With hydrogen peroxide as the oxidizer, the cycle is analyzed with JP-7 and ethanol as fuels. With hydrazine as the fuel, nitrogen tetroxide is the only oxidizer considered in the analysis, as the hydrogen peroxide/hydrazine combination has a lower vacuum specific impulse of 302 s. Two drawbacks of the decomposition cycle are that it requires an extra combustion chamber and that in each case, one propellant drives the other's turbopump. With inadequate sealing, this could lead to combustion in the pump. An advantage of the system is that decomposition is sure to take place on start-up. The hydrogen peroxide/ethanol, hydrogen peroxide/JP-7, and nitrogen tetroxide/hydrazine decomposition topping cycles are examined in more detail in section 3.2.

3.1.2 Expander Cycle

The expander cycle uses the heat absorbed in the coolant to drive the turbopumps. The heat from the cooling passages is added to the fluid after it exits the pump. Figure 3-2 shows a schematic of the expander cycle.

The expander cycle has an advantage of simplicity since it only has one combustion chamber. The following propellant combinations are considered: hydrogen peroxide/ethanol, hydrogen peroxide/JP-7, nitrogen tetroxide/ethanol, nitrogen tetroxide/hydrazine, and nitrogen tetroxide/Aerozine 50. Aerozine 50 is a 50/50 mixture of hydrazine and UDMH. The nitrogen tetroxide/ethanol cycle is attractive, because it is clear that both the fuel and oxidizer can be used as coolants and to drive their own pumps, so there is no danger of the propellants mixing before they reach the chamber. However, the maximum frozen flow vacuum I_{sp} of the combination with an expansion ratio of 15 is found to be 296 s. This ideal performance is considered too low, so this combination is not considered further. The nitrogen tetroxide/hydrazine expander cycle is examined in more detail in section 3.2.

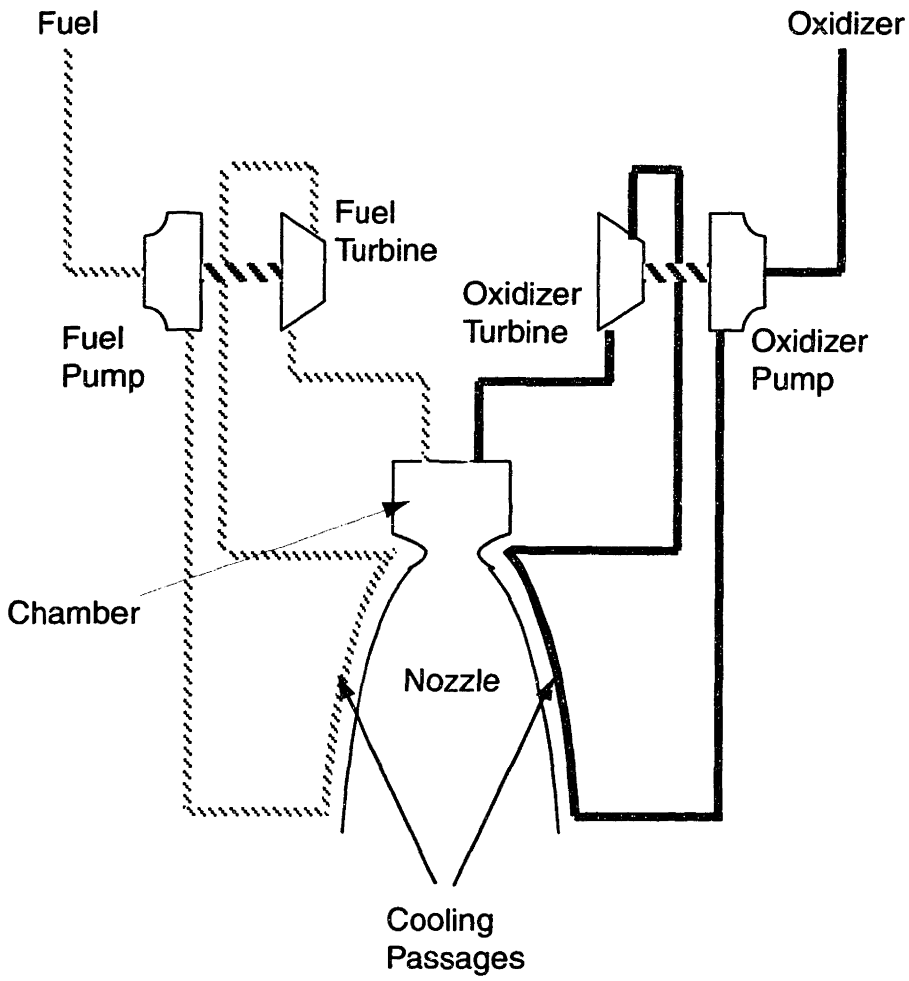

Figure 3-2: Expander Topping Cycle Flow Paths and Components.

3.1.3 Gas-Generator

The gas-generator cycle is an auxiliary combustion cycle. The turbine gas is generated in a separate chamber. The cycle is shown schematically in figure 3-3. The turbine gases are generated by combining the propellants at a mixture ratio that that is different from the optimum. This yields a lower combustion temperature than in the main combustion chamber because not all of the fuel in a fuel rich process burns and likewise for an oxidizer rich process. A non-optimal mixture ratio is chosen in order that the pre-combustion chamber temperature is kept below the turbine inlet temperature limitations. This cycle differs from the decomposition cycle where only one propellant is used to generate gas to drive the turbines. In the cycle shown, the turbine gas is exhausted

overboard through a smaller nozzle. This results in a performance loss, as these propellants are not combined at the ideal oxidizer to fuel ratio.

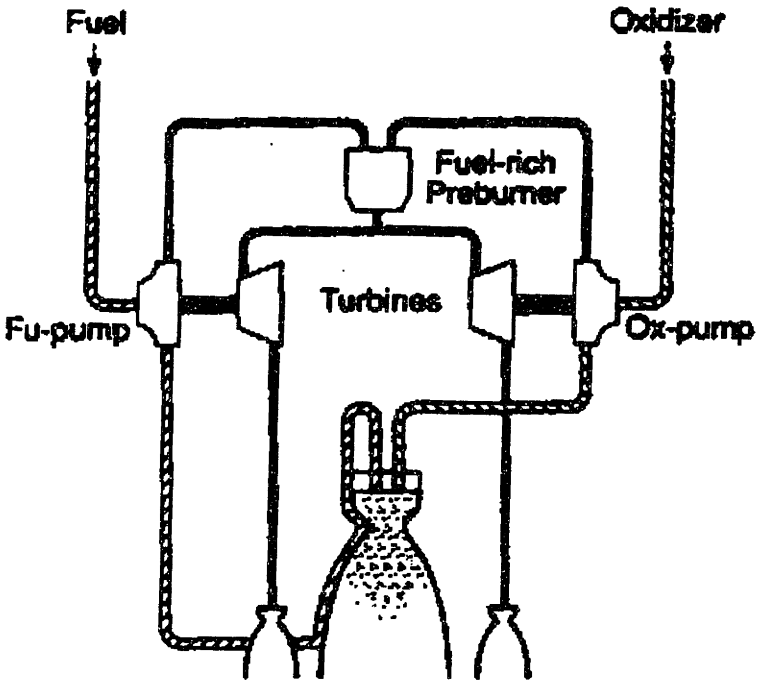

Figure 3-3: Fuel-Rich Gas-Generator Cycle [Manski].

3.1.4 Other

Other possibilities for engine cycles are presented below.

Figure 3-5 shows the fuel-rich staged combustion cycle. In this cycle all of the propellants are routed through the main combustion chamber. In the cycle shown, both a fuel-rich and oxidizer rich precombustor are used. Only one may be necessary, but using both prevents leaks in either turbopump from reacting with its turbine gas. These properties of this cycle make it attractive.

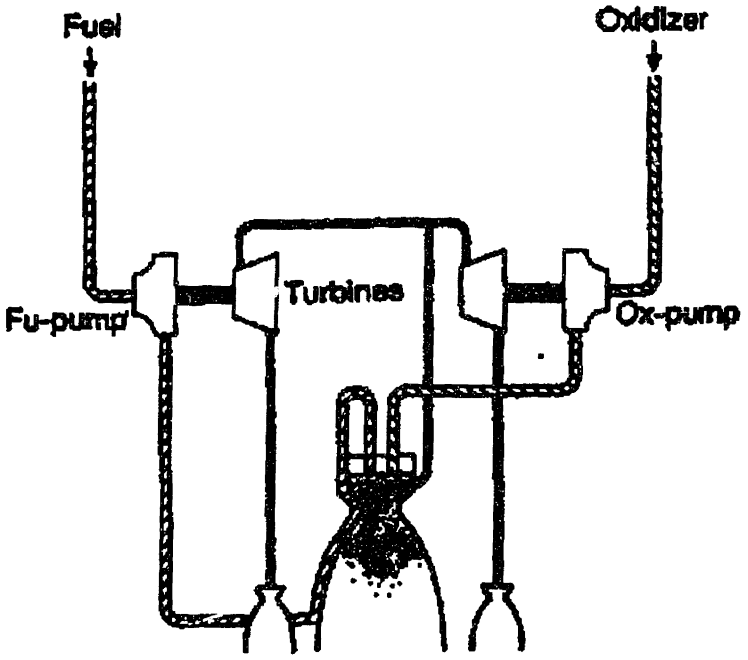

Figure 3-4: Fuel-Rich Tap-Off Cycle [Manski].

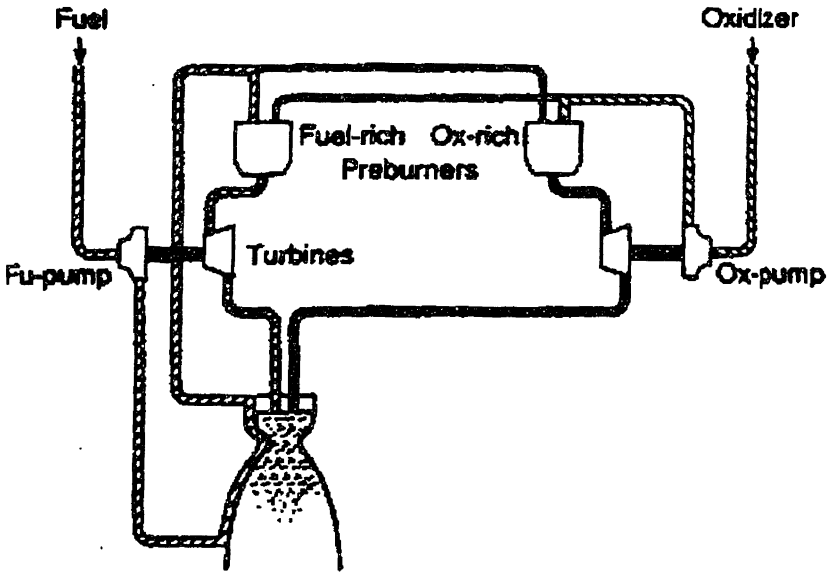

Figure 3-5: Simple Full-Flow Staged Combustion Cycle with Oxidizer- and Fuel-Rich Preburners [Manski]

These last three cycles are not examined further because they are deemed to be too complex at the present time. They do, however, offer options to parts of the cycles presented above. For example the cycles above could be modified to dump the turbine exhaust overboard. This results in a drop in specific impulse, and is to be avoided if possible. Figure 3-4 shows a tap-off cycle. In this cycle, the gas to drive the turbines is extracted from the chamber. With film cooling in the chamber, the temperature of the tap-off gas can be kept below maximum allowable turbine inlet temperature. In the micro-rocket engine, film cooling is not presently employed, and the temperature in the chamber is difficult to determine, so this cycle is not considered. This cycle dumps the turbine gas overboard as shown by the smaller nozzles.

3.2 Decomposition Topping Cycle

The decomposition topping cycle is shown in Figure 3-1. Liquid hydrogen peroxide or hydrazine is pumped to high pressure and fed through cooling passages and into the gas generator or decomposition chamber. This chamber contains a catalyst. The catalyst material is yet to be determined, but is discussed in section 4.3. The catalyst speeds the decomposition of the propellant, resulting in high temperature gaseous products, steam and oxygen in the case of the hydrogen peroxide and N_2, H_2, and NH_3 in the case of the hydrazine. These gases drive the turbopumps. The turbine exhaust passes through the injectors into the main chamber where it combines with the complement propellant. The propellant not used for decomposition is pumped to high pressure and fed through a different set of cooling passages and into the main chamber.

The adiabatic decomposition temperature of the decomposition products of hydrogen peroxide is approximately 1100 K. The energy in the products is enough to cause the fuel and oxygen to react without the aid of igniters, thus reducing the complexity of the system [McCormick].

In the case of hydrazine decomposition, the oxidizer, nitrogen tetroxide, and the fuel are hypergolic, again eliminating the need for igniters. This system design requires a second chamber that may have to be cooled (see chapter 2). The major challenge in the

decomposition chamber is providing the required chamber surface area for catalysis. This is discussed briefly in section 4.

3.2.1 Power Requirements

The decomposition cycle is required to produce enough power to pump the propellants through the cooling passages, decomposition chamber, turbine (for the hydrogen peroxide or hydrazine), and injectors. The power required to pump the propellants to a given pressure, assuming incompressible fluids can be written,

$$P_{pump} = \dot{m}\Delta H = \dot{m}\frac{\Delta P}{\rho} \tag{3.1}$$

This power can also be approximated as,

$$P_{pump} = \dot{m}\eta_p(\omega r_p)^2 \tag{3.2}$$

P_{pump} is the pumping power, $\dot{m}$ is the mass flow through the pump, ΔH is the enthalpy change of the fluid, ΔP is the pressure change across the pump, ρ is the liquid density, ω is the rotational speed of the pump, r_p is the radius of the pump, and η_p is the pump efficiency. The power required must be less than the power produced by decomposition of the hydrogen peroxide, since this is the source of the power for the pumps. The enthalpy after decomposition, which is the turbine inlet enthalpy can be found starting from the equation for the Isp of a monopropellant thruster,

$$I_{sp} = \frac{c}{g} = \left(\frac{1}{g}\right)\sqrt{2C_pT_1\left[1-\left(\frac{p_e}{p_c}\right)^{\frac{\gamma-1}{\gamma}}\right]} \tag{3.3}$$

The monopropellant Isp's of hydrogen peroxide and hydrazine thrusters at a chamber pressure of 100 psi are 147 s and 250 s respectively [Sutton]. The power provided by the turbine is [Kerrebrock, 1992],

$$P_{turb} = \dot{m}_t\Delta H_t = \dot{m}_t C_p T_1\left(1-\frac{T_2}{T_1}\right) \tag{3.4}$$

Or

$$P_{turb} = \dot{m}_t C_p T_1\eta_t\left[1-\left(\frac{p_2}{p_1}\right)^{\frac{\gamma-1}{\gamma}}\right] \tag{3.5}$$

The inlet enthalpy, CpT_1, is known from equation 3.3, and the pressure ratio can be adjusted to fit the desired combustion chamber pressure and pump outlet pressure, developed in the following sections.

3.2.2 Pumping System Analysis Assumptions

The fluid pumped is assumed to be incompressible, so the power it requires can be written as in equation 3.1. This assumption is valid because the oxidizer and fuel are liquid propellants at standard temperature and pressure, so they will both be liquid as they enter and exit the pump.

The decomposition chamber outlet enthalpy is assumed to be equal to the turbine inlet enthalpy and is found from the monopropellant thrust relation and from measurements of the specific impulse of monopropellant hydrogen peroxide and hydrazine thrusters. The specific impulses used are 147s for hydrogen peroxide and 250 s for hydrazine thrusters at a chamber pressure of 100 psi. The pressure ratio is 14.7/100 [Sutton].

The efficiency of the pump and turbine is each assumed to be 0.5. This is based on an estimate from the MIT micro gas turbine engine development [Epstein].

The pressure drop in the cooling passages of the gaseous micro-rocket engine has been calculated to be 50 atm for a chamber pressure of 125 atm and a cooling passage inlet pressure of 300 atm [London, 1999]. This pressure drop is 17 percent of the pressure at the entrance to the cooling passages, and 40 percent of the chamber pressure. A typical pressure loss for cooling jackets is between 5 and 20 percent of the chamber pressure [Sutton]. A fixed cooling channel pressure drop of 50 atm is chosen for this analysis. This assumption is valid at the desired chamber pressure of 125 atmosphere and it not as reasonable for chamber pressures much higher or lower than this.

3.2.3 Pressure Requirements

The cycles analyzed must be able to sustain a chamber pressure of 125 atm. This means that the turbopumps have to deliver enough power to pump the propellants to the chamber pressure plus the injector pressure drop plus the cooling passage pressure drop plus the turbine pressure drop.

This analysis is performed assuming a pressure drop of twenty percent across the injector. In the micro-rocket it may be desirable to operate with choked injectors. This would ensure that there is no communication between the chamber and elements of the system upstream of it.

The cooling passages are designed to meet the cooling requirements, so the propellants will necessarily lose pressure in these passages. The pressure drop in the cooling passages is estimated to be at least 50 atm for a cooling passage entrance pressure of 300 atm [London, 1999].

3.2.4 Valid Operating Range

Figure 3.6 (a) shows the results for the hydrogen peroxide decomposition cycle. Pump outlet pressure and chamber pressure, P_c, are plotted against the turbine pressure ratio. The turbine pressure ratio necessary to supply the pump power is shown on the x-axis. The upper line shows the pump outlet pressure necessary to reach this chamber pressure given the above assumptions and the chamber pressure and expansion ratio on the chart. Any chamber pressure less than 200 atm is achievable, but as the chamber pressure rises, the pump outlet pressure rises faster. The results are summarized in the table below.

Table 3-1: Pump Outlet Pressure and Turbine Pressure Ratio Resulting from a Chamber Pressure of 125 atm for Decomposition Cycles.

	O/F Ratio	$\dot{m}$ [g/s]	$\dot{m}$ Decomposition [g/s]	Pump Outlet Pressure [atm]	Turbine Pressure Ratio []
JP-5/H_2O_2	5.8	5.21	4.44	253	0.77
Ethanol/H_2O_2	4.0	5.75	4.60	261	0.74
Hydrazine/N_2O_4	1.2	5.28	2.40	243	0.81

The turbine inlet temperature is predicted to be 1600K (see section 2.4 above). This temperature is important for the structural design of the turbine, however it is not necessary for these calculations because the enthalpy in the decomposition propellant is known, and this sets the valid operating range. That is, with a constant specific heat, the change in temperature of the decomposition products is fixed for the given design point. The temperature of the propellants at the exit of the cooling passages (see section 2.3 and 2.4 above) does not influence the valid operating ranges below.

Since the decomposition cycles are shown to be viable using all of the available decomposition propellant it is possible that only a fraction could be used to drive the turbomachinery. This fraction could enter the decomposition chamber without going through the cooling passages, so the decomposition chamber temperature would be 1100K. However, all of the propellant is necessary for cooling, and with a lower mass flow through the turbine, the turbine pressure ratio would necessarily be lower, and a higher pump outlet pressure would result. This possibility has not been examined in further detail.

The results for the hydrazine decomposition cycle are shown in figure 3-7, and are also summarized with the hydrogen peroxide decomposition cycles results in Table 3.1 above.

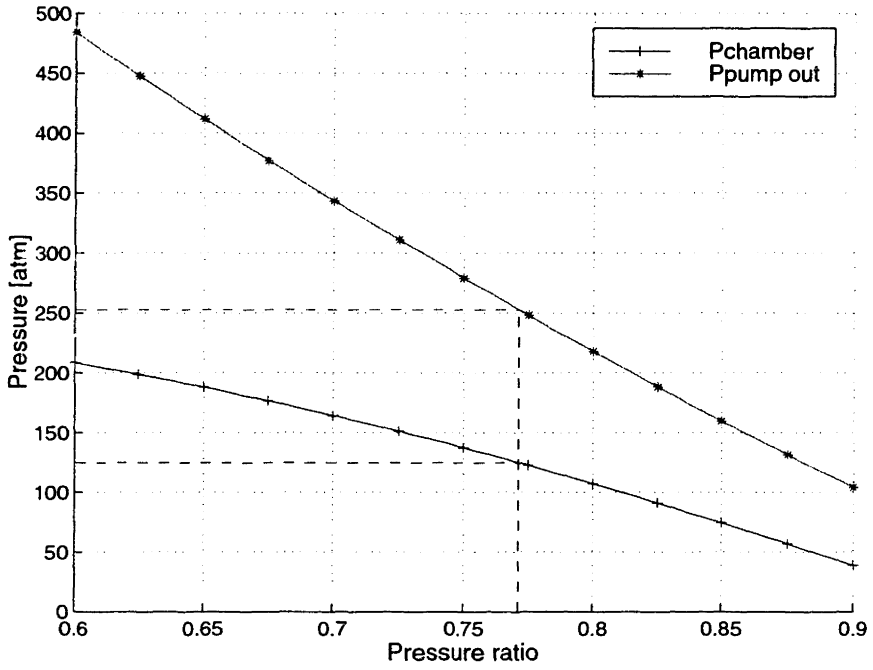

(a)

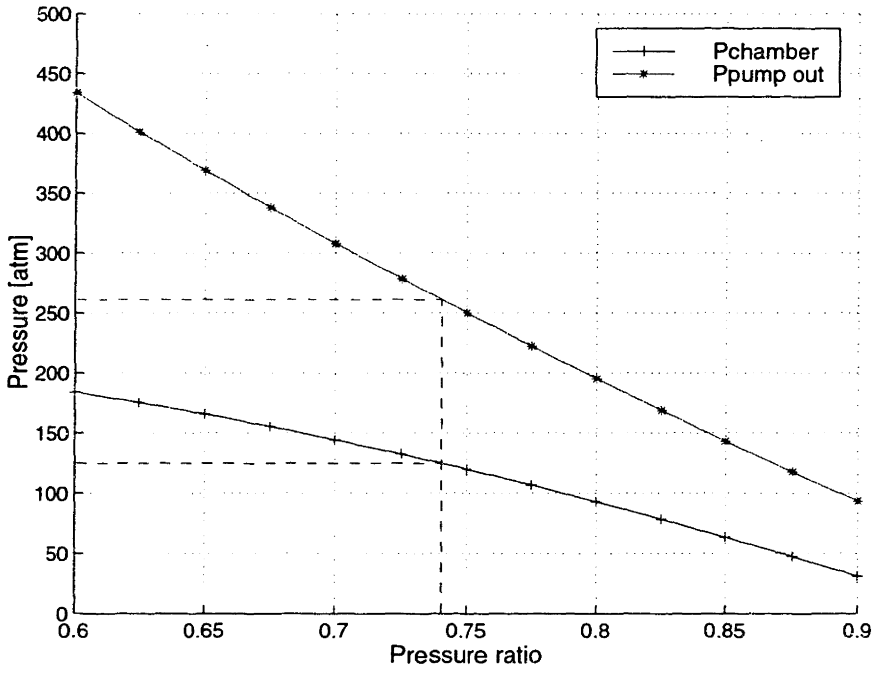

(b)

Figure 3-6: Cycle Analysis Results for **(a)** Hydrogen Peroxide/JP-7 Cycle and **(b)** Hydrogen Peroxide/Ethanol Cycle.

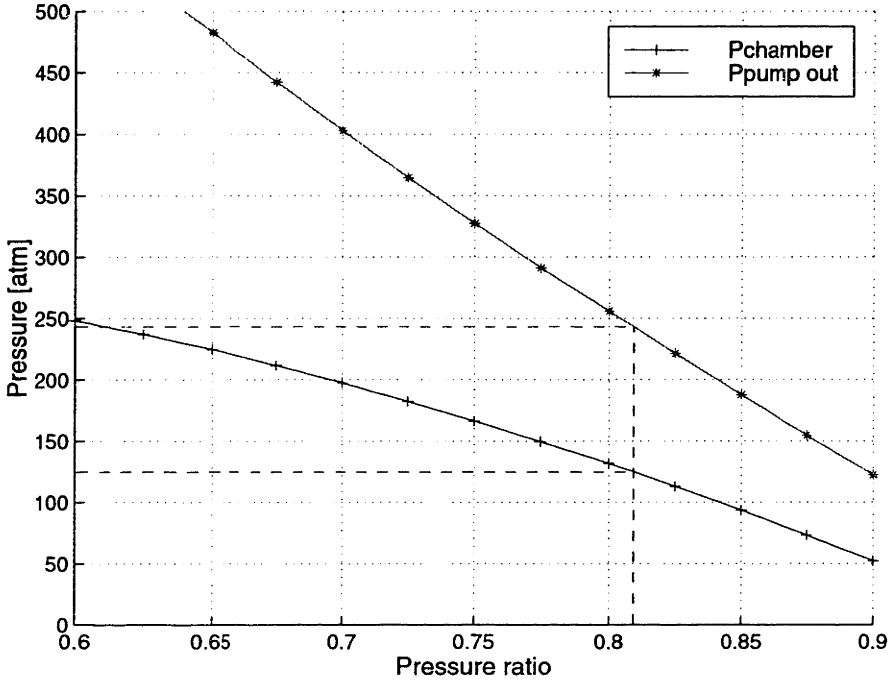

Figure 3-7: Hydrazine/Nitrogen Tetroxide Decomposition Cycle Analysis Results.

3.3 Expander Cycle

The expander cycle is shown in figure 3-2. The propellants are pumped to high pressure. They then pass through the cooling passages, where they pick up the heat necessary to drive the turbines. The propellants then expand in the turbine and are injected into the combustion chamber. A notable feature of this cycle is that each propellant can be used to drive its own pump. This eliminates the chance of explosion if hypergolic propellants were to leak from the pump side to the turbine side if the sealing was inadequate. The fuel side and oxidizer side expander cycles are analyzed independently below.

3.3.1 Power Requirements for Expander Cycle

The expander cycle for each propellant is required to produce enough power to pump the propellant through the cooling passages, turbine, and injectors. The power required to pump the propellants to a given pressure, assuming incompressible fluid, was

shown in equation 3.1. The power required to pump the propellants to this pressure must be less than the rate at which propellants absorb heat in the cooling passages. The method for finding the total heat absorbed is detailed in Chapter 2. The power extracted from the turbine is found from equation 3.5. The inlet enthalpy is known from the heat absorbed in the coolant, and the pressure ratio can be adjusted to fit the desired combustion chamber pressure resulting in the pump outlet pressure. These results are shown after a discussion of the assumptions, and the pressure requirements of the system.

3.3.2 Pumping System Analysis Assumptions

The pump is assumed to be incompressible, so the power it requires can be written as in equation 3.1. This assumption is valid because the oxidizer and fuel will both be liquid as they enter and exit the pump.

The efficiencies of both the pump and turbine are each assumed to be 0.5 [Epstein].

The pressure drop in the cooling passages of the gaseous micro-rocket engine has been calculated to be 50 atm for a chamber pressure of 125 atm and a cooling passage inlet pressure of 300 atm [London, 1999]. This pressure drop is 17 percent of the pressure at the entrance to the cooling passages, and 40 percent of the chamber pressure. A typical pressure loss for cooling jackets is between 5 and 20 percent of the chamber pressure [Sutton]. A fixed cooling channel pressure drop of 50 atm is chosen for this analysis. This assumption is valid at the desired chamber pressure of 125 atmosphere and it not as reasonable for chamber pressures much higher or lower than this.

The heat that the propellants must absorb is assumed to be split between them based on the oxidizer to fuel ratio. The heat that each propellant absorbs is determined by the cooling passage design. This design could ensure that the propellants each reach the same temperature after the cooling passages or that they reach the same pressure at the turbine exhaust (see chapter 2).

3.3.3 Pressure Requirements

The expander cycle has pressure requirements similar to those of the decomposition cycle.

3.3.4 Valid Operating Range

The results for the nitrogen tetroxide/hydrazine expander cycle are shown in figures 3-8, 3-9, and 3-10. Figure 3-7 shows the results for the maximum predicted heat load the propellants must absorb, 8541W. Figure 3-9 shows the results for a heat load of 4781W. Figure 3-10 shows the results for the minimum predicted heat load the propellants must absorb, 2699W. Although the temperatures of the propellants do fall below their critical temperatures, their pressure is always above the critical pressure, so there is no possibility of a phase change in the turbine. The turbine inlet temperatures below are found from the temperature-enthalpy curve of the propellants (see Table 2-9).

Table 3-2: Pump Outlet Pressure and Turbine Pressure Ratio Resulting from a Chamber Pressure of 125 atm for Expander Cycles at $r = 1.2$ and $\dot{m} = 5.28$ g/s.

	Heat Load [W]	Turbine Inlet Temperature [K]	Turbine Exit Temperature [K]	Pump Outlet Pressure [atm]	Turbine Pressure Ratio []
N_2O_4	8541	705	682	242	0.86
Hydrazine	8514	839	806	248	0.84
N_2O_4	4781	502	478	256	0.78
Hydrazine	4781	650	615	261	0.79
N_2O_4	2699	434	410	265	0.78
Hydrazine	2699	528	491	278	0.73

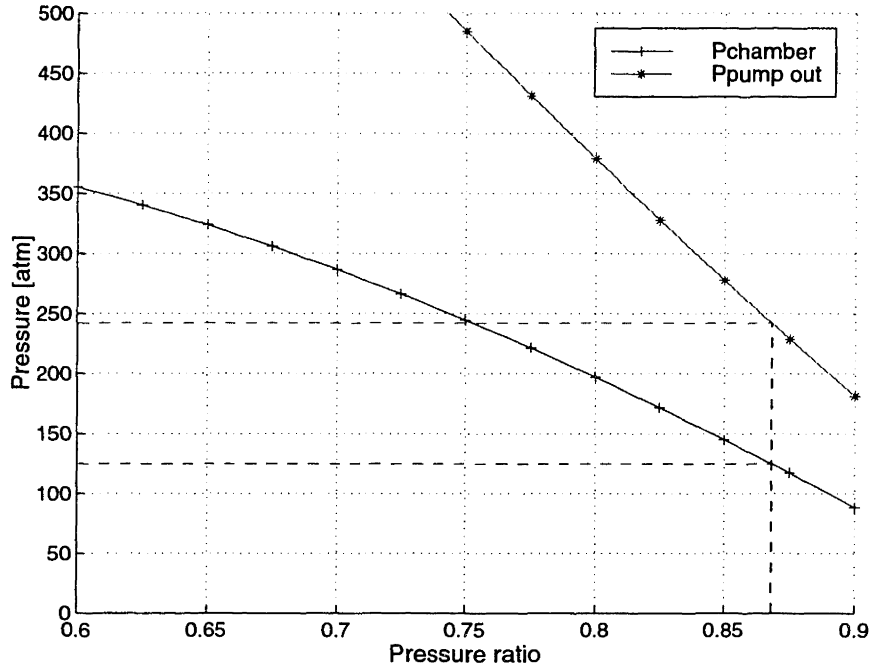

(a)

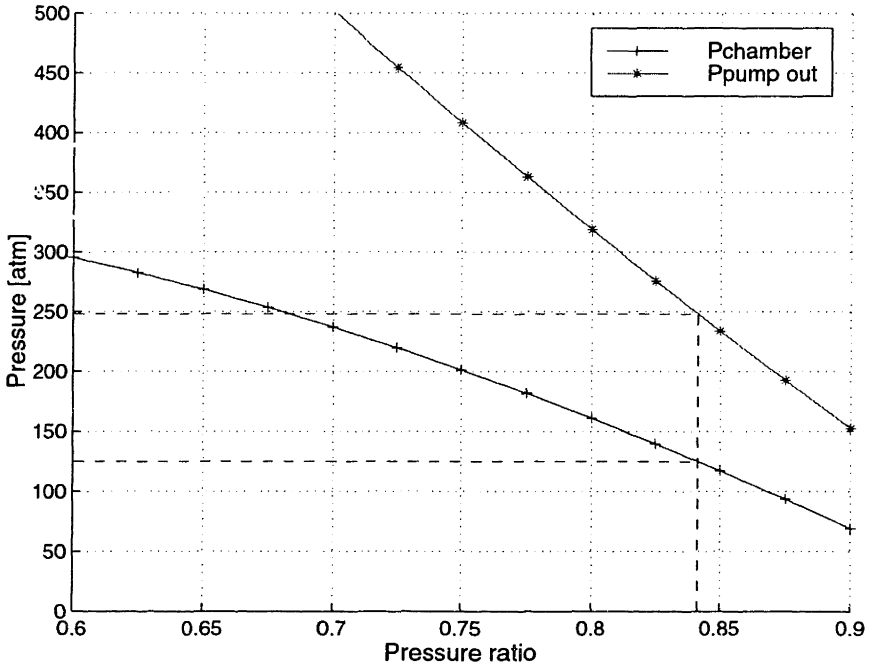

(b)

Figure 3-8: Cycle Analysis Results for the Nitrogen Tetroxide **(a)** and Hydrazine **(b)** Expander Cycle Assuming a Heat Load of 8541 Watts.

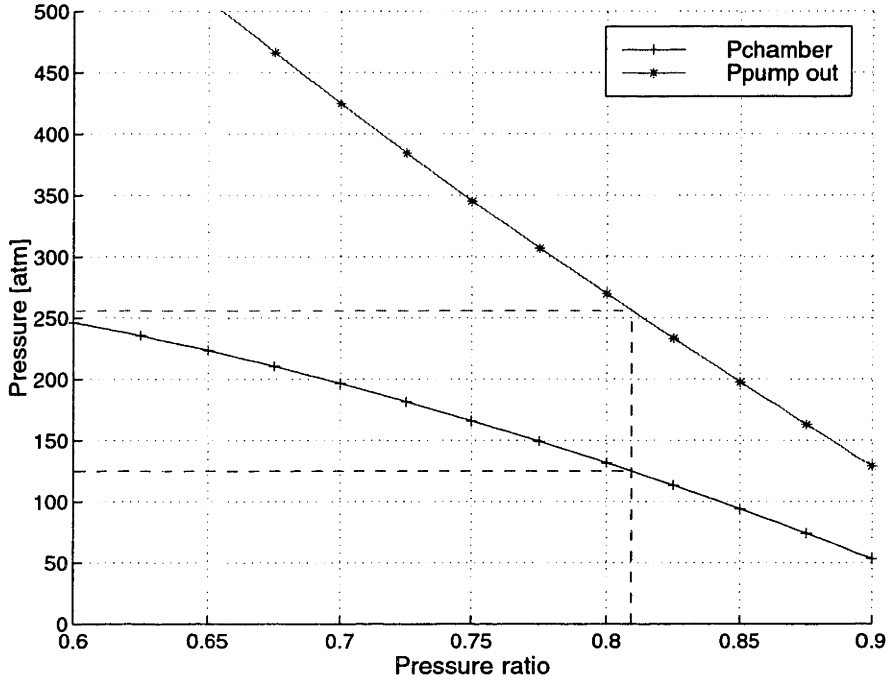

(a)

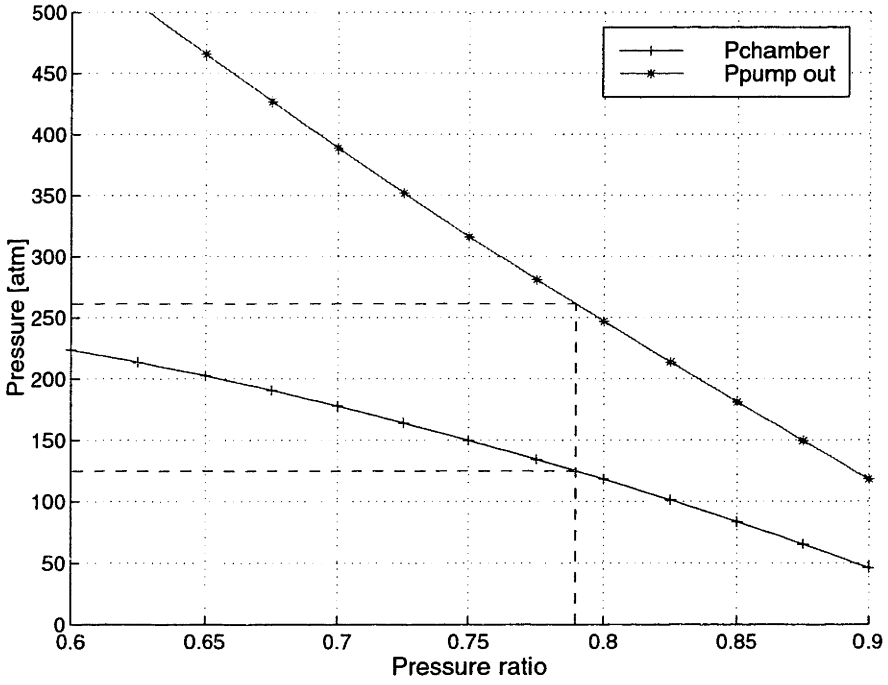

(b)

Figure 3-9: Cycle Analysis Results for the Nitrogen Tetroxide **(a)** and Hydrazine **(b)** Expander Cycle Assuming a Heat Load of 4781 Watts.

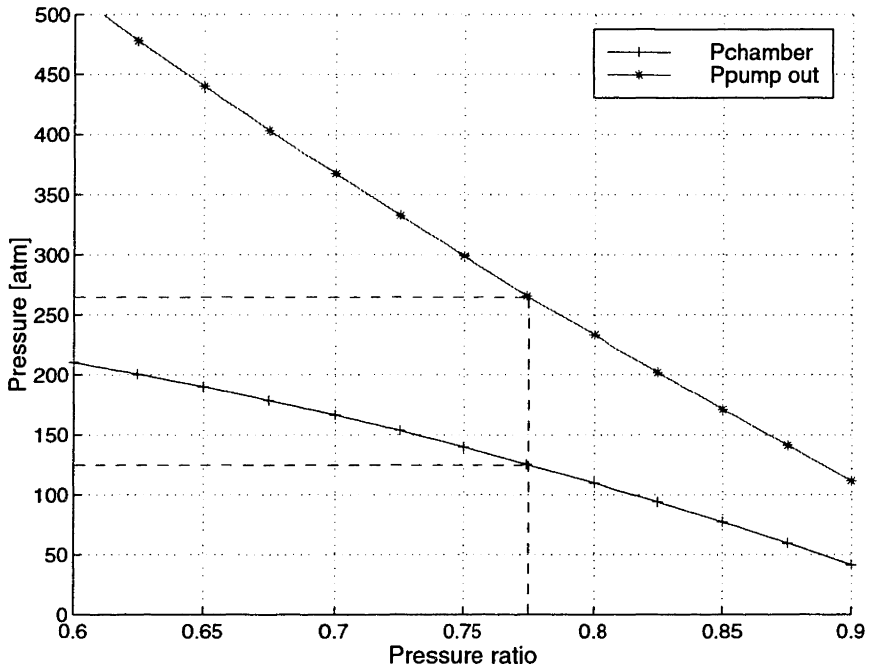

(a)

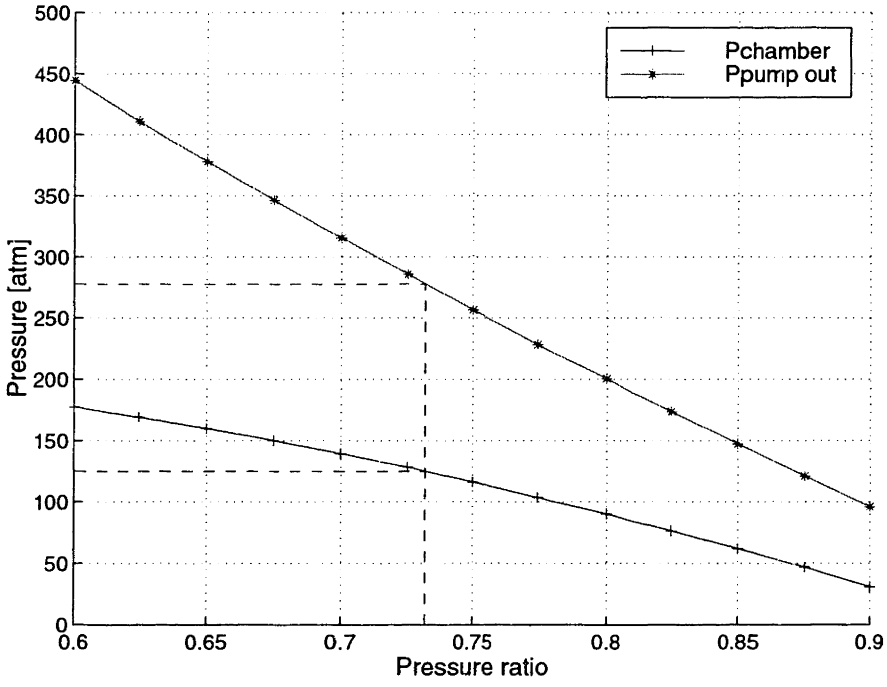

(b)

Figure 3-10: Cycle Analysis Results for the Nitrogen Tetroxide **(a)** and Hydrazine **(b)** Expander Cycle Assuming a Heat Load of 2699 Watts.

3.4 Cycle Conclusions

The results shown above indicate that the hydrogen peroxide/ethanol, hydrogen peroxide/JP-7, and nitrogen tetroxide/hydrazine decomposition topping cycles and the nitrogen tetroxide/hydrazine expander cycles are all viable cycles at a chamber pressure of 125 atm.

The expander cycle has the advantage that each propellant is used to drive its own pump and turbine. The propellants cannot mix until they enter the combustion chamber. This is especially important with hypergolic propellants. However, the design of the expander cycle relies on the knowledge of the change in enthalpy of the cooling fluid. As mentioned in Chapter 2 above, these estimates are not accurate, presently. Experimental data is necessary.

The decomposition cycles have the advantage that the enthalpy released by the monopropellant is established and is insensitive to errors in approximating the final propellant temperature after the cooling channels. The major disadvantages with this cycle are that a decomposition chamber would have to be developed and integrated, and that decomposition products would be used to drive the complement propellant's turbopump. With a hypergolic combination (and all the decomposition combinations examined are), a leakage from the pump would burn in the turbine.

CHAPTER 4

COMPONENTS

4.1 Introduction

The components that make up the micro-rocket system are summarized. A summary of the work conducted as part of separate research efforts is presented on several of the components. A preliminary analysis is presented on the pump and bearings. An introduction to the requirements for the controls and valves of the system is presented.

4.2 Main Chamber

Work has been performed on the main chamber as part of a separate research effort. The main chamber provides the necessary volume for the propellants to mix and react in. The gas temperature in the main chamber will be approximately 3000K. To maintain the strength necessary to withstand the chamber pressure, the chamber walls in the given design must be kept below 900 K (see figure 4.1 below). This is accomplished with a regenerative cooling scheme mentioned in Chapter 2.

The structure of the chamber must be able to withstand pressures greater than 125 atm. This means that the bonds between the chamber wafers must be strong enough to withstand this pressure, too. A structural analysis was performed and chambers have been fabricated and pressure tested validating the strength of the current design [London, 1999].

Figure 4.1 shows the strength versus temperature curves of silicon and silicon carbide. For a given stress level, these curves show the maximum temperature the material can be used at. This temperature is important because it sets the cooling requirements for the main combustion chamber and the decomposition chamber. The figure also shows that if silicon carbide were used in these chambers, the wall temperature could be raised significantly. This would mean the propellants would have to absorb less heat or that the chamber temperature and thus pressure could be raised resulting in better engine performance. Processes for microfabricating silicon carbide structures are not yet fully developed, though.

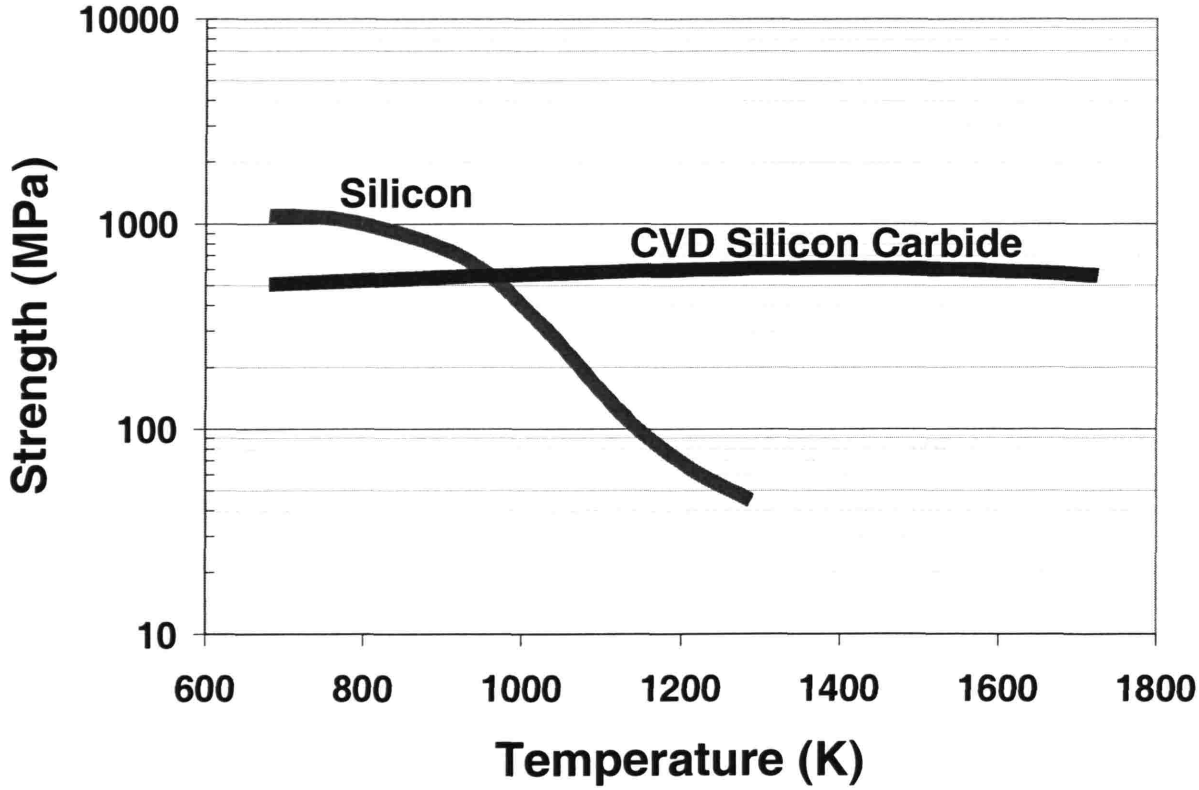

Figure 4-1: Strength versus Temperature for Silicon and CVD Silicon Carbide [Courtesy Kevin Lohner].

A more detailed analysis of the nozzle, injector, and main chamber design can be found in London, 1999.

4.3 Cooling System

The primary purpose of the cooling system is to keep the chamber and nozzle walls at temperature lower than the combustion chamber temperature. This temperature is determined by material properties including strength and oxidation rate.

The internal design of the cooling passages is based on the local heat flux. The pressure drop in the channels is also a design consideration. The channels must be designed with the proper surface area and heat transfer coefficient to match the local heat flux. As size of the channel is decreased, for a given mass flow, the volumetric flow rate, (ρu) must rise, resulting in a higher heat flux. The size, or width, of the channel can only be decreased to the minimum feature size that can be manufactured. The design must be able to cool the throat, the area of the engine with the highest heat flux. To achieve the necessary heat transfer coefficient, features have been designed and implemented in the current design [London, 1999]. An example of simple structures to increase the area, and the heat flux since qdot~hA, is the fins shown in Figure 4-1.

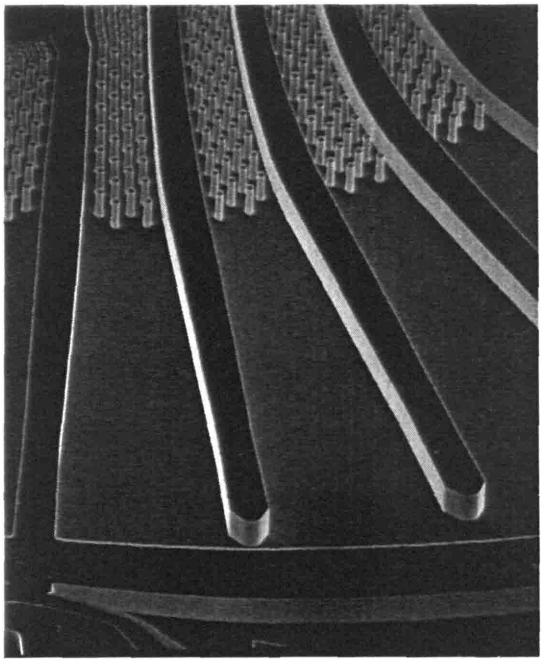

Figure 4-2: Throat Top Wall Cooling Passages and Fins [Courtesy Adam London, 1999].

These fins can only be etched on the top and bottom cooling walls, since features can mainly be microfabricated perpendicular to the plane of the wafer. An example of vertical features that increase the heat transfer coefficient is the turbulators used near the throat shown in Figure 4-3.

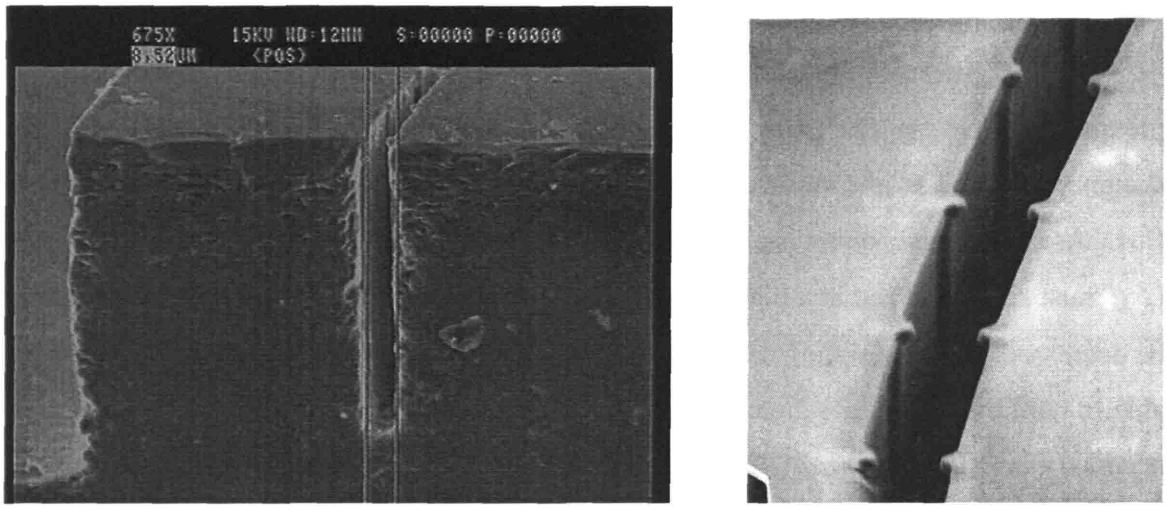

Figure 4-3: Throat Cooling Passage Cross Section Showing Turbulators [Courtesy Adam London, 1999].

Film cooling techniques are often applied in rocket engines to keep the wall temperature at acceptable levels. In this technique, coolant is injected along the chamber walls making a fuel or oxidizer rich region that has a much lower temperature than the rest of the chamber. These techniques are a possibility in later builds of the micro-rocket.

4.4 Decomposition Chamber and Catalyst

The decomposition chamber is necessary for the decomposition cycles mentioned above. It provides the large surface area of catalyst necessary to decompose the propellant in a given length. In large-scale monopropellant engines, the catalyst surface area is obtained by forcing the propellant through mesh screens of the catalyst metal [McCormick]. In a micro-rocket engine, structures similar to the top wall cooling passage fins in figure 4-2 could be coated with a catalyst, because the microfabrication technique makes it easy to fabricate a large number of repeated structures. A micro scale catalyst enhanced reaction chamber has been developed already by the MIT Chemical

engineering department [Franz]. The catalyst is applied to fins in the chamber by spraying an aerosol mixture through the chamber. The chamber has been shown to catalyze reactions, but it does have a large pressure drop [Franz].

The decomposition chamber thermal constraints are not as severe as the main combustion chamber constraints, but they are important. As discussed in chapter 2, the hydrogen peroxide decomposition cycle does not have enough cooling capacity in the fuel alone, and the decomposition chamber would have to be cooled. Experimental results are necessary to determine if the main chamber and nozzle walls in the nitrogen tetroxide/hydrazine decomposition chamber must be cooled (see chapter 2).

To fabricate a decomposition chamber a catalyst would have to be deposited on the silicon substrate. Deposition is a process that accomplishes this and is frequently employed in microfabrication. Deposition does not pose much of a problem in itself, however it has been mentioned that silicon tends to neutralize the catalyzing effects of silver [Schmidt]. Fortunately, several metals and compounds can be deposited through microfabrication techniques, and "most impurities act as a catalyst" [Sutton]. Some other candidate catalysts include copper, manganese dioxide, iron oxide, and, platinum [McCormick, Sutton]. The decomposition chamber design is an area that needs further research to ensure that the catalyst is compatible with silicon, and that complete decomposition occurs.

4.5 Turbomachinery

Centrifugal pumps are used to bring the propellants to the required pump discharge pressure. Figure 4-1 shows a concept for micro turbopumps. The pump is on the top, the turbine on the bottom, and a bearing gap in-between the two. This section discusses these three components.

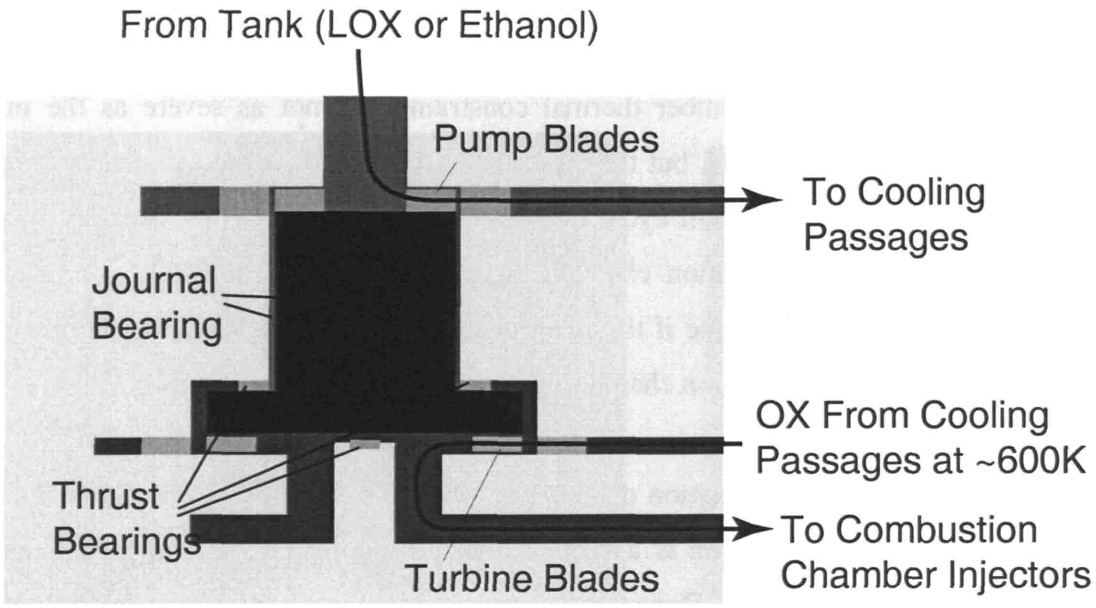

Figure 4-4: Turbopump concept cross-section [Courtesy Omar Al-Midani].

4.5.1 Pumps

These pumps must have enough strength to survive the high rotational speeds necessary to pump the fluid. The pumps will drive fluid at about 300K, and are assumed to be isothermal devices. However, because of the high thermal conductivity of silicon, 125W/m^2/K, heat from the turbine will be conducted to the pump through the shaft. This heat transfer may cause a problem with cavitation in the pump.

Using the Euler turbine equation and assuming that the density of the propellant is constant, a valid assumption, since it is liquid, the tip speed required to pump a given propellant to a certain pressure can be approximated as in equation (3-2). The outer radius of the pump is set by the blade height and desired propellant mass flow, and is found from:

$$\dot{m} = \rho u A = \rho u \left(2\pi r_p h_b\right) \tag{4-1}$$

where u is the radial velocity of the fluid at the pump exit.

4.5.1.1 Pump Specifications

The design of the initial compressor of the MIT micro gas turbine engine is used to evaluate whether the current design will be able to meet the required pressure rise for the micro rocket engine system. The following analysis shows that the present design is indeed capable of meeting the requirements. The analysis is also useful for determining the tank pressure required to ensure that the pump does not cavitate.

The ten-blade design analyzed is shown in Figure 4-5. This figure shows the representation of the blades used in the MISES viscous/inviscid multiple blade cascade analysis / design system. MISES is a compressible code. The analysis was initially performed on a water pump that reaches a pressure of 100 atmosphere [Jacobsen].
An inlet Mach number of 0.1 is selected to ensure that Mach numbers in the pump are kept below 0.1, so that the flow remains incompressible. Since the Mach number ratio is roughly proportional to the area ratio of the passage, the Mach number will never exceed 0.28. The outer radius of the pump is 2.8 times the inner radius.

$$\frac{\rho_0}{\rho} = \left(1 + \frac{\gamma - 1}{2} M^2\right)^{\frac{1}{\gamma - 1}} \tag{4-2}$$

With the ratio of specific heats, γ = 1.3, the density ratio is 1.05. The actual density differs from the stagnation density, the density of an incompressible fluid, by 5% at most. The MISES output is reduced to determine what the pumping characteristics for an incompressible liquid would be. To reduce the calculations, first, a geometry is chosen to meet the desired mass flow as described above. The two variables that can be manipulated for the chosen bladeset are the outer radius, *r2*, and the blade height, *b*, shown in Figure 4-6. The rest of the geometry is then defined.

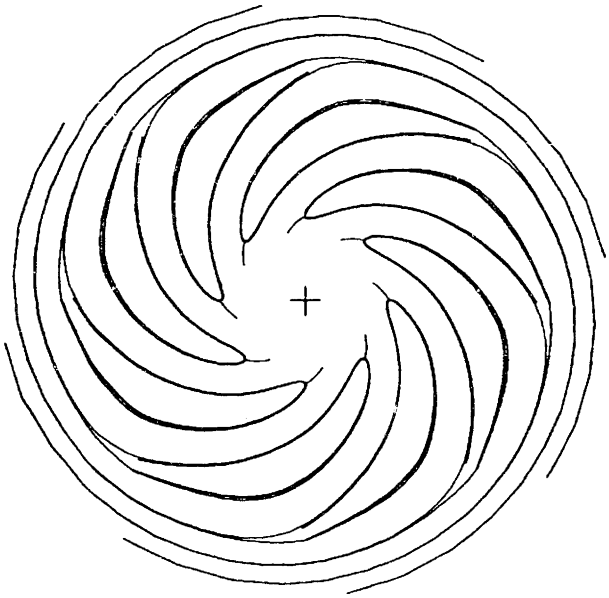

Figure 4-5: MISES Representation of Pump Wheel [Jacobsen].

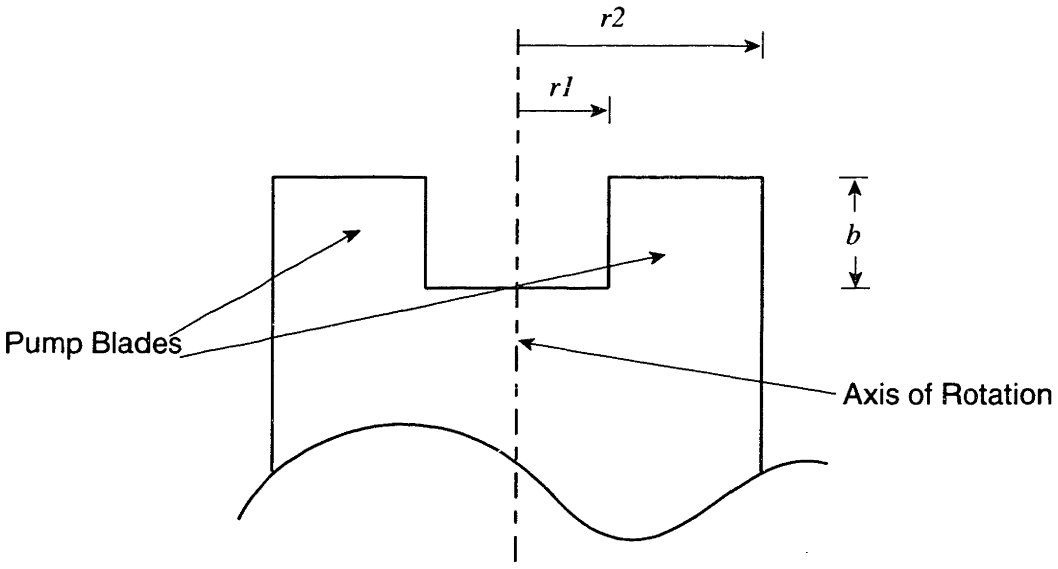

Figure 4-6: Pump Nomenclature.

Then, a pressure and temperature are selected for the air using the ideal gas law, $P=\rho RT$, where ρ is the density of the propellant being considered. The tip speed of the

pump is then selected so that the nondimensional tip speed, rotrel, matches the MISES input, where

$$rotrel = \frac{\omega r_p}{\sqrt{\gamma RT}} \tag{4-3}$$

The estimated pressure rise in the pump is chosen based on the tip speed selected above. The inlet mach number is compared to 0.1, the input value, and the outlet mach number is compared to the MISES output. Finally, the selected ΔP is compared to the actual ΔP found by

$$\Delta P = P_1\left(\frac{P_2}{P_1}\right) - P_1 \tag{4-4}$$

where the pressure ratio is found from MISES. This process is repeated until the liquid values converge to the MISES output. The properties of the liquid pump can then be found. This process is completed for five liquid propellants. First, the MISES output for the 100 atm water pump is reduced for each propellant. The results are shown in Table 4-1.

Table 4-1: 100 atm Water Pump Results Reduced for Chosen Propellants.

Propellant	ΔP [atm]	$\dot{m}$ [g/s]	Re []	ω [rad/s]	r1 [mm]	r2 [mm]	b [mm]
Hydrazine	107	22.5	10800	190000	0.66	1.84	0.2
Ethanol	83	31	10800	110000	1.1	3.2	0.2
JP-7	86	35	10800	96000	1.3	3.6	0.2
Nitrogen Tetroxide	152	10	10800	600000	0.21	0.57	0.2
Hydrogen Peroxide	154	31	10800	200000	0.64	1.8	0.2

The analysis is then repeated. This time the MISES inputs are modified to reach a pump output pressure of 300 atm for each propellant. The mass flow guesses are chosen based on a 5 g/s system, and each propellant is weighted by its o/f ratio from Table 2-3. The hydrogen peroxide mass flow guess is set to the hydrogen peroxide/JP-7 oxidizer to fuel ratio for simplicity. The results are shown in Table 4-2.

Table 4-2: ~300 atm Pump results for Chosen Propellants.

Propellant	ΔP [atm]	$\dot{m}$ [g/s]	Re []	ω [rad/s]	r1[mm]	r2 [mm]	b [mm]
Hydrazine	220	8.0	29000	590000	0.12	0.33	0.23
Ethanol	210	5.0	15000	780000	0.1	0.28	0.2
JP-7	200	6.7	15000	600000	0.12	0.34	0.24
Nitrogen Tetroxide	280	5.6	63000	770000	0.08	0.23	0.17
Hydrogen Peroxide	280	6.1	21000	650000	0.1	0.27	0.19

The small pump radii shown above indicate that it may be easier to develop a micro-rocket with a higher mass flow so that the turbomachinery components could be larger.

4.5.1.2 Pump Cavitation

In turbopumps it is important that the blades of the pump do not cavitate. Cavitation occurs when the local pressure on the surface of the blade falls below the vapor pressure of the liquid. This results is local vaporization of the liquid. Cavitation usually occurs behind the leading edge of the blade on the suction side of the airfoil. As the bubbles travel downstream, they encounter higher pressure and collapse back to the liquid state. These fluctuations along the blades can result in flow and combustion instabilities. Cavitation can also result in erosion of the surface of the blades, but this is usually less important due to the short duration of the rocket firing, however on 25 micrometer blades, cavitation deterioration of the blades is important. Combustion instabilities can have catastrophic effects, so cavitation is to be avoided [Sutton]. Cavitation can be eliminated of the local pressure of the flow never reaches the vapor pressure. The MISES results showing the pressure coefficient profile along a hydrazine pump blade is shown in Figure 4-7. It can be seen that the minimum Cp is ~ –0.8.

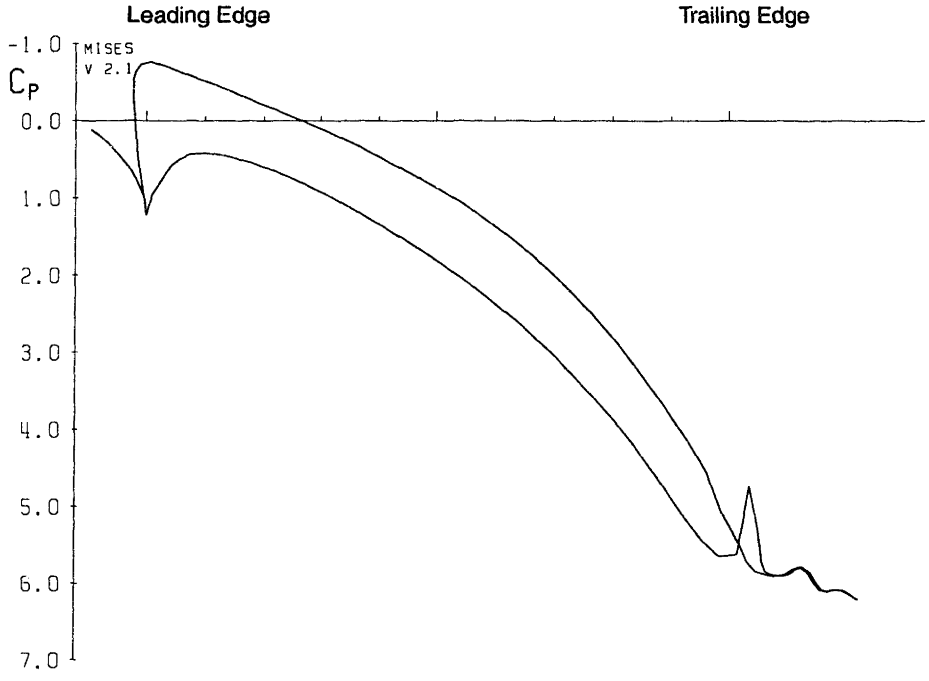

Figure 4-7: Pressure Coefficient on Pressure and Suction Sides of Hydrazine/Nitrogen Tetroxide Pump Blade

$$C_p = \frac{p - p_\infty}{\frac{1}{2}\rho v_\infty^{\,2}} \tag{4-5}$$

Setting p equal to the vapor pressure at this minimum Cp location the tank pressure, p_∞, necessary to eliminate cavitation is found. The results are summarized in table 4-3.

Table 4-3: Minimum Pump Inlet Pressure for Chosen Propellants

	Minimum Pump Inlet Pressure [atm]
Ethanol	22.3
Hydrogen Peroxide	27.9
JP-7	19.8
Hydrazine	26.0
Nitrogen Tetroxide	34.7

These pressures are relatively large compared to a more typical tank pressure of 5 atm [Sutton]. This indicates that the blades must be redesigned to lower the minimum pressure on the blade surface. The tank pressures could also be reduced if a booster pump is installed before the main fuel and oxidizer pumps. The booster pump has a

smaller ΔP, so the minimum Cp on the blades is lower, and less tank pressure is required to prevent cavitation. The flow is then at a high enough pressure to prevent cavitation when it enters the main pumps, too.

4.5.2 Turbines

Turbines are used to provide the required shaft power to the pumps. The turbine must also provide power for losses that occur in the bearings and seals of the engine. They do this by expanding gas through nozzles and vanes to convert the enthalpy of the fluid to kinetic energy. Turbine design has already been considered as part of a separate research project [Al-Midani, Epstein].

4.5.3 Bearings

The micro-rocket bearing is divided into a thrust bearing to balance the forces due to pumping the liquid and driving the turbine, and a journal bearing to separate the spinning elements from the stationary ones. The thrust bearing is a fluidic bearing. It relies in pressure and area differences to keep the spinning machinery centered vertically. The micro-rocket thrust bearing design will be based on the micro-gas turbine thrust bearing, which has been successfully operated [Epstein].

The journal bearing is also a fluidic bearing. It consists of the rotating shaft, or cylindrical journal, between the pump and turbine, a stationary wall outside of the shaft, or annular sleeve, and a bearing gap between the two. It is shown above in figure 4.1. The bearing gap is filled with propellant bled from the pump output. Because the pump outlet pressure is around 300 atm, the fluid entering the bearing is supercritical for all the propellants examined. It is treated as a gas with the viscosity found in references [Primex, FMC, Pillori, USAF, Kakac, Barin]. The fluid journal bearing can be operated either hydrodynamically or hydrostatically. In hydrodynamic operation, the bearings rely on highly nonlinear pressure differences in the bearing gap. In this mode of operation, the bearing obtains stiffness from these pressures generated as the fluid is forced around

the gap by viscous drag. In hydrostatic operation, the bearing stiffness is obtained simply by forcing high pressure fluid radially into the bearing gap.

The operation and stability of the journal bearing is critical to the operation of the engine system. First, it is considered how much power is lost in the bearing gap due to viscous drag. The flow is assumed to have no pressure variation in the circumferential direction, and is analyzed as Couette flow. This gives the shear stress as

$$\sigma = \mu \frac{\partial U_{wall}}{\partial y} \cong \mu \frac{U_{wall}}{h} \tag{4-6}$$

and $U_{wall} = \omega r_p$ and h, the fluid passage height is equal to the bearing clearance, c.

The drag power is then

$$P_d = U_{wall} A \sigma_d = 2\pi\mu \frac{b}{c} \omega^2 r_p^3 \tag{4-7}$$

where b is the bearing height. With μ~0.001 Pa·s, $b \sim r_p$~300um, ω ~ 700000rad/s, and c~10um, this yields P~2 Watts, not a large fraction of the roughly 100 Watts needed to pump each propellant.

Second, a numerical stability analysis of the hydrodynamic journal bearing stability is found in [Al-Midani]. The governing equations for this type of journal bearing may not be solved analytically with sufficient generality. [Hamrock]. It is found that side loading must be applied to the bearing to keep the eccentricity high enough to generate the stabilizing forces required. These results show that for liquid oxygen and ethanol, only 2% of the pump impeller area needs to be subjected to higher pressure to generate the stabilizing side load. Given that the pump speeds and radii required to pump hydrogen peroxide, JP-7, nitrogen tetroxide, and hydrazine are similar to those for liquid oxygen and ethanol, and that the viscosities of all these propellants are greater than that

of liquid oxygen, and less than that of ethanol, this analysis shows that this type of bearing is feasible for these propellants, also.

It is possible that hydrostatic bearings could be implemented in the micro-rocket, but research has not been conducted in this area.

4.6 Controls

All liquid rocket engines require controls. The control systems can range from simple valves to start the rocket engine to complicated systems to vary the mixture ratio of the propellants to utilize all the propellants on board. The application and requirements are important factors in determining the complexity of the control system of a rocket engine. Sutton states,

> All liquid propellant rocket engines have controls to accomplish some or all of the following tasks:
> 1. Start rocket operation.
> 2. Shut down rocket operation
> 3. Restart, if desired.
> 4. Maintain programmed operation (predetermined constant or randomly varied thrust, preset propellant mixture ratio and flow).
> 5. When safety devices sense an impending malfunction or a critical condition of the vehicle or the engine then the control system will automatically change conditions or cause an emergency engine shutdown.
> 6. Fill with propellants
> 7. Drain excess propellant after operation
> 8. Check out proper functioning of critical components or a group of components without actual hot operation before and/or after flight
> 9. For recoverable and reusable rocket engines also provide built-in self-test features to perform continuous checks in flight and on the ground and recycle the engine to a ready condition within a few minutes after a launch abort without any ground servicing.

At the minimum, the controls for the micro-rocket engine must provide controls to start the rocket operation. This includes bringing the turbomachinery to operating pressures and mass flows and igniting the propellants in the chamber. Igniters can be eliminated from the system if the propellant combination is hypergolic, and the propellant

combinations and cycles being considered are hypergolic. Turbopump-fed rocket engines have been started in a variety of ways. Sutton lists three common ones:

1. A solid propellant start grain or start cartridge is used to pressurize the gas generator, and this starts turbine operations. . .This is usually the fastest start method, but it does not provide a restart.
2. This method, known as tank head start, is used on the SSME, is slower, does not require a start cartridge, and permits engine restart. The head of the liquid from the vehicle tanks (usually in vertically launched large vehicles) causes a small initial flow of propellants; then slowly more pressure is built up as the turbine begins to operate and in a couple of seconds the engine "bootstraps" its flows and pressures to their rated values.
3. A small auxiliary pressurized propellant feed system[s] is used to feed the initial quantity of fuel and oxidizer (at essentially full pressure) to the thrust chamber and gas generator.

For the micro-rocket engine, the "bootstrap" method is favorable. This method reduces the system complexity, since no auxiliary pressurized propellant feed system or solid propellant start grain is necessary.

The engine may be able to maintain programmed operation passively. If the injector area is sized properly, the mass flow of each of the propellants will be kept at the prescribed values at the operation point of the engine. The oxidizer to fuel ratio will not be kept constant during startup due to the differences in physical properties of the propellants. A separate control may be necessary to maintain the proper mixture ratio to eliminate the possibility of flame blow-out or combustion instabilities at startup.

Safety controls in the micro-rocket engine would protect personnel and the vehicle. These controls would ensure that the main valves remain closed while the vehicle is being handled, and default to the closed position if power is lost. These safety controls reduce the risk of explosion, and are especially important for hypergolic propellant combinations. The controls must provide a safe situation for fueling the rocket and draining unused propellants left in the tanks. One way to reduce the complexity of the controls is to have the entire device assembled with the tanks filled at the factory. This only works for a single-shot device, though.

Most controls on rocket engines use a servomechanism principle. The variable or quantity to be controlled is measured by a sensing device, and its value is compared to the desired value by a computing or controlling mechanism. The controlling mechanism gives a signal to the actuating device, which changes the variable being controlled [Sutton]. Controls of this design require sensing devices. These devices typically measure turbopump rotational rate, mass flow of propellants or pressures at proscribed locations. Controls of this sort would be required to set the thrust of the micro-engine at a desired level, below the maximum, i.e. to throttle the engine.

Liquid rocket control actuation functions are usually achieved through valves, regulators, pressures switches, and flow controls. The requirements for these devices are briefly discussed in the next section.

4.7 Valves

The design and fabrication of micro-scale valves is a complicated task in itself. These devices must be able to provide the necessary functions for control of the engine, and at the same time they must be small enough not to add much weight to the system. A large valve would diminish the advantageous thrust to weight ratio of the micro-rocket engine.

At least two actuating devices are needed for any cycle considered. If these devices are valves, they are the main valves that separate the propellant tanks from the rest of the system. These valves provide the safety functions mentioned above and enable engine start through the bootstrap method. These valves can also be used to control the mass flow of each of the propellants. This would allow for throttling of the engine, as lower mass flow levels would produce lower thrust. If these valves are controlled separately, the controller could also change the oxidizer to fuel ratio of the engine to ensure that both tanks empty at the same time. These two valves are necessary, and they are also sufficient for the minimum level of control of the engine. These valves would have to provide sealing between the tanks, which are at 25 atm and 300K, and the

rest of the system which is initially at 1 atm and 300K. These valves would also provide shutdown capability to the engine. It is also desirable for the valves to have intermediate settings between full open and full closed to allow for engine throttling.

Another possible actuating device is a burst diaphragm. These diaphragms can be used alone to replace the main control valves or in series with them. First, they could be used alone. They would only provide the ability to start the engine. Shutdown, throttling, and restart are not possible with diaphragms alone. Second, diaphragms could be used in series with valves to provide the initial sealing of the engine, so the valves would only have to modulate the mass flow of the propellants. Finally, the diaphragms could be used along with the valves mentioned above that could shutdown the engine. The diaphragms would provide safety during transportation and handling by ensuring that the propellants could not mix.

4.8 Summary

Thrust chambers, injectors, and cooling passages for gaseous pressure-fed micro-rockets have been designed and successfully demonstrated as part of a separate research effort [London, 1999]. These components must be redesigned for a liquid micro-rocket. Preliminary analysis shows that the present fluidic design of the micro-gas turbine engine could pump liquid propellants to 300 atm. To prevent cavitation it must be redesigned specifically for liquids. Preliminary analysis also shows that liquid micro-bearings will work in micro-turbopumps. Research is being conducted on the analysis of liquid micro-bearings [Deux]. Further work is necessary to develop a valve layout and control scheme for the micro-rocket.

CHAPTER 5

CONCLUSION

The micro-rocket system is analyzed in this thesis. It's applications and advantages are discussed early. The significant reduction in propulsion system weight leads directly to weight savings in the vehicle. More payload can be delivered or maintained at the same cost resulting in a significant cost savings.

A summary of the research conducted for this thesis is presented. This summary includes research conducted to determine a propellant combination and cycle that will meet the requirements for the device and maintain the high performance of liquid bipropellant systems. It also includes work to show that the components of the system will be able to meet their requirements. Recommendations and discussion of future work necessary in the project follow.

5.1 Summary of work

5.1.1 Propellant Combination

The storable liquid bipropellant micro-rocket system is analyzed. The requirements for the system are presented. Cycle and propellant alternatives are examined based on these requirements.

Propellant combinations are evaluated primarily on their specific impulse. Properties such as cooling capacity, toxicity, whether or not the combination is hypergolic, and whether or not the propellant can be catalytically decomposed are also considered. Three propellant

combinations are chosen for further analysis: nitrogen tetroxide, hydrazine, hydrogen peroxide/JP-7, and hydrogen peroxide/ethanol. The combination of hydrazine and nitrogen tetroxide is chosen because of it's high Isp (322s, see Chapter 2) which makes it a popular combination in engines today, and because hydrazine can be catalytically decomposed. The combination of JP-7 and Hydrogen Peroxide also chosen. While its specific impulse in the micro-rocket design (318s) is not as great as that of Hydrazine and nitrogen tetroxide, it is a "non-toxic" combination, and hydrogen peroxide can also be catalytically decomposed. The hydrogen peroxide/ethanol combination appears to be the best choice to carry to the next phase of the project. Although it only provides 302s of Isp, both propellants are non-toxic, neither propellant etches silicon, and ethanol has been proven as a coolant in micro-machined silicon passages.

5.1.2 Cycle Analysis

Several candidate cycles are considered. A preliminary group of cycles is chosen based upon their simplicity and performance. Closed cycles, those that inject the turbine exhaust into the chamber, are favored because in general they have better efficiencies than cycles in which the exhaust is dumped overboard. Four cycles are analyzed: hydrogen peroxide/JP-7 decomposition, hydrogen peroxide/ethanol decomposition, nitrogen tetroxide/hydrazine decomposition, and nitrogen tetroxide/hydrazine expander. All of these cycles are shown to meet the pressure requirements of the system. The decomposition topping cycle is suggested for future work because the hydrogen peroxide/ethanol propellant combination is chosen, there is less uncertainty in the start-up of this cycle, and the pump performance is not directly tied to the cooling system design.

5.1.3 Components

Key features of Thermal, Mechanical, Fluid, and Fabrication of each major component are presented. The combustion chamber and injectors, decomposition combustion chamber, cooling system, pumps, turbines, bearings, controls, and valves are presented. Key areas of the components are analyzed to ensure feasibility and find operational space.

The pumps are analyzed to find the required pumping power. Given the requirements for mass flow and the chamber and cooling system pressures, the pump is sized. The viscous losses in the bearing gap are found to be less then 3% of the pumping power. A pump bladset is analyzed to determine the tank pressure necessary to prevent cavitation. The required tank pressure is found to be between 20 and 30 atm. Preliminary considerations indicate that the micro-turbopump bearing will be stable. However, a more comprehensive analysis of the bearing is needed to fully validate the concept.

The combustion chamber, decomposition chamber, and cooling system are examined. The cooling passages have been designed to meet the heat load, however it is not unusual for actual heat fluxes to differ by a factor of two from the heat fluxes determined with correlations. Tests in the near future will determine whether or not the mixing and cooling scheme are adequate. Additional analysis and design is required for liquid combustion chambers, injectors, and the decomposition chamber and catalyst, but research has shown that decomposition chambers can be manufactured at the micro-scale.

Key requirements of the micro-rocket control system and valves are presented. The most important is the rocket start sequence. Tank head start is the recommended start method. More detailed analysis of the control system is required.

5.2 Recommendations and Future Work

Recommendations based on the research presented and plans for future work required for project completion are detailed below.

5.2.1 Recommendations

A detailed analysis and characterization of the pumping system is required. This involves turbomachinery design and test. The aerodynamics of the pump and turbine must be evaluated,

and the bearing stability must be proven. One step toward this goal would be to test the micro-engine compressor as a water pump. This would provide data on the pumping characteristics to compare with the MISES code and useful data on liquid bearings. The option to employ hydrostatic bearings should also be examined.

Finally, the design of the chamber must be modified and tested for liquids and for the specific propellant combination chosen. This includes changing the injectors and a redesign of the cooling system.

5.2.2 Future Work

The following is a list of the research endeavors required to drive the project to completion.

- Analysis of launch vehicles employing micro-rockets: This effort, currently underway, will show if small launchers are feasible and cost effective. A systems design of a launcher will be completed.

- Characterization of water heat transfer rates at high heat fluxes and high pressures: This effort, currently underway, will validate the previous ethanol heat transfer experiments and verify the performance of the test rig as well as provide insight on cooling passage design specifications. This rig may be used in the future to test the propellants chosen for the micro-rocket engine.

- Fabrication, assembly, and test of a gaseous pressure-fed micro-rocket: This effort is also currently underway. The pressure fed chamber, injectors, nozzle, and cooling channels shown in Figure [1-2] will be fabricated and assembled. This device will then be tested. This effort will show the effectiveness of the injection and cooling scheme, as well as provide data on the actual thrust produced by the device.

- Turbomachinery design: A detailed design of the pumps and turbines required for the micro-rocket is required. This design will include the size, blade geometry, and bearing geometry. These elements will be tested separately initially and possibly connected by pipes to a chamber later as an initial test of the chamber and turbomachinery operating together.

- Control and valve development: The micro-rocket control system must be designed, and the technology to produce the valves that serve as the control actuators must be developed or borrowed, if it is available.

- Integration of the chamber, turbomachinery, and controls: After each element of the system is developed, they must be integrated into a single micro-rocket engine unit.

- Testing and design re-iteration: These steps will be performed at various stages of the product development. Some testing is mentioned above, and design re-iteration would take places after the results of these tests are evaluated.

APPENDIX A

This appendix presents tables and figures showing the CEA results of the same propellant combinations presented above at the conditions shown in Table A-1. The two differences are that the flow is assumed to be in chemical equilibrium throughout the chamber and nozzle, and it is expanded to atmospheric pressure.

There are two differences in the ordering of the combinations by specific impulse. First, the nitrogen tetroxide/JP-5 combination has the same performance as the nitrogen tetroxide/hydrazine combination and second, the nitrogen tetroxide/JP-5 cycle has better performance than the hydrogen peroxide/JP-5 cycle. There is no difference in the ranking ordering of the combinations by density specific impulse.

Table A-1: Chamber and Nozzle Parameters Used in Propellant Performance Analysis.

Chamber Pressure	125 atm
Chamber Area: Throat Area	16:1
Nozzle Area: Throat Area	15:1
Back Pressure	1 atm
Oxidizer Inlet Temperature	298.15 K
Fuel Inlet Temperature	298.15 K

Table A-2: Maximum Chemical Equilibrium Specific Impulse and Associated Chamber Temperature and Oxidizer to Fuel Ratio of Selected Propellant Combinations.

	O/F Ratio	Chamber Temperature	Isp [s]	Id [g*s/m^3]
Hydrazine/N_2O_4	1.3	3301	308	378
Hydrazine/H_2O_2	2.0	2946	302	383
JP-5/N_2O_4	3.6	3640	302	374
JP-5/H_2O_2	6.2	3133	298	389
Ethanol/N_2O_4	2.6	3299	284	332
Ethanol/H_2O_2	4.2	2912	286	354

Table A-3: Maximum Chemical Equilibrium Density Specific Impulse and Associated Chamber Temperature and Oxidizer to Fuel Ratio of Selected Propellant Combinations.

	O/F Ratio	Chamber Temperature [K]	Isp [s]	Id [g*s/m^3]
Hydrazine/ N_2O_4	1.4	3315	308	380
Hydrazine/ H_2O_2	2.0	2946	302	383
JP-5/ N_2O_4	4.0	3669	301	377
JP-5/H_2O_2	7.0	3116	297	391
Ethanol/ N_2O_4	3.0	3310	281	335
Ethanol/ H_2O_2	4.4	2906	286	356

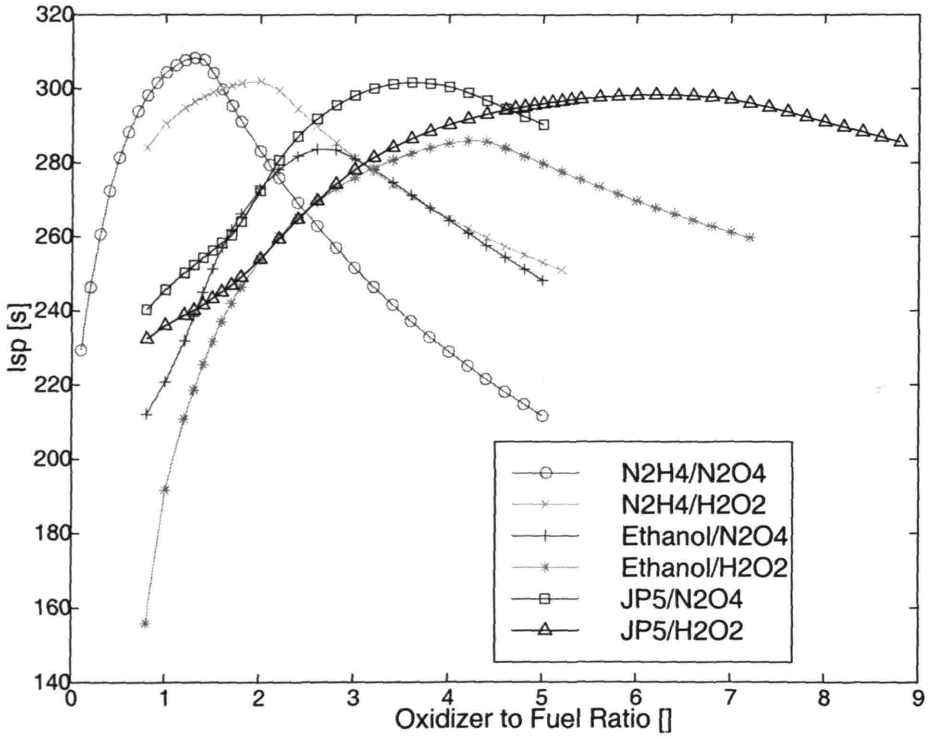

Figure A-1: Specific Impulse vs. Oxidizer to Fuel Ratio of Selected Propellant Combinations Assuming Chemical Equilibrium.

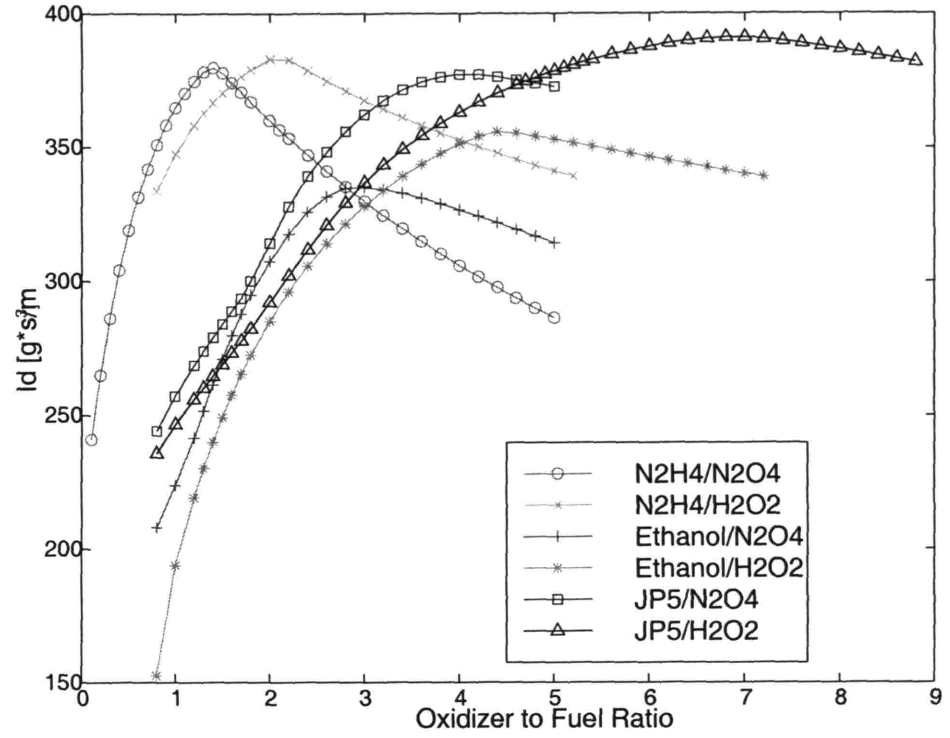

Figure A-2: Density Specific Impulse vs. Oxidizer to Fuel Ratio of Selected Propellant Combinations Assuming Chemical Equilibrium.

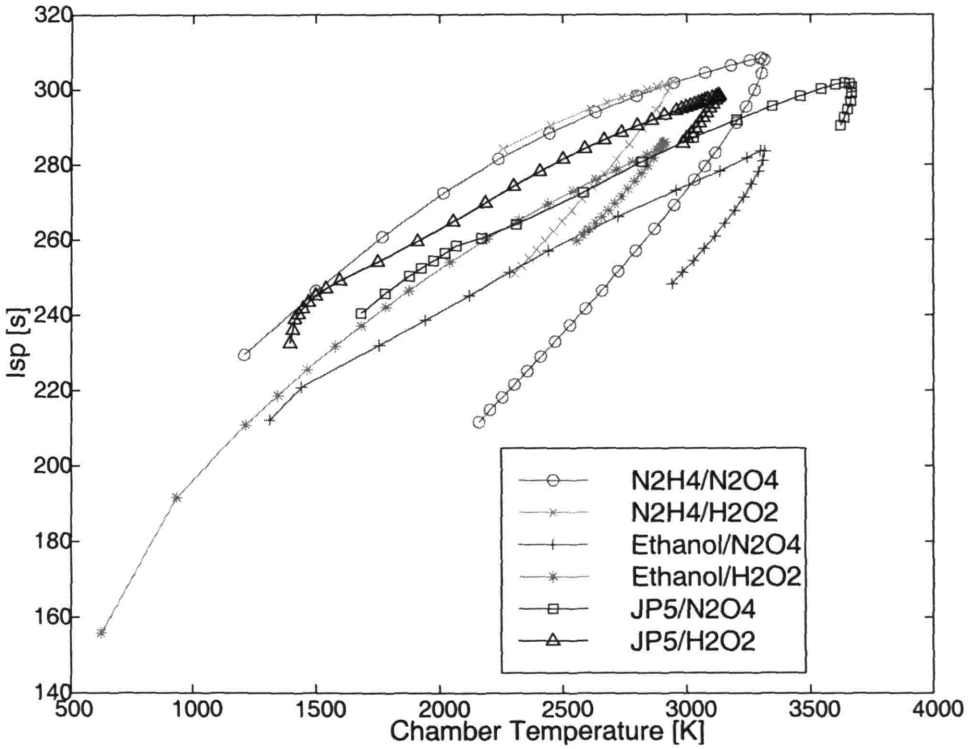

Figure A-3: Specific Impulse vs. Chamber Temperature of Selected Propellant Combinations Assuming Chemical Equilibrium.

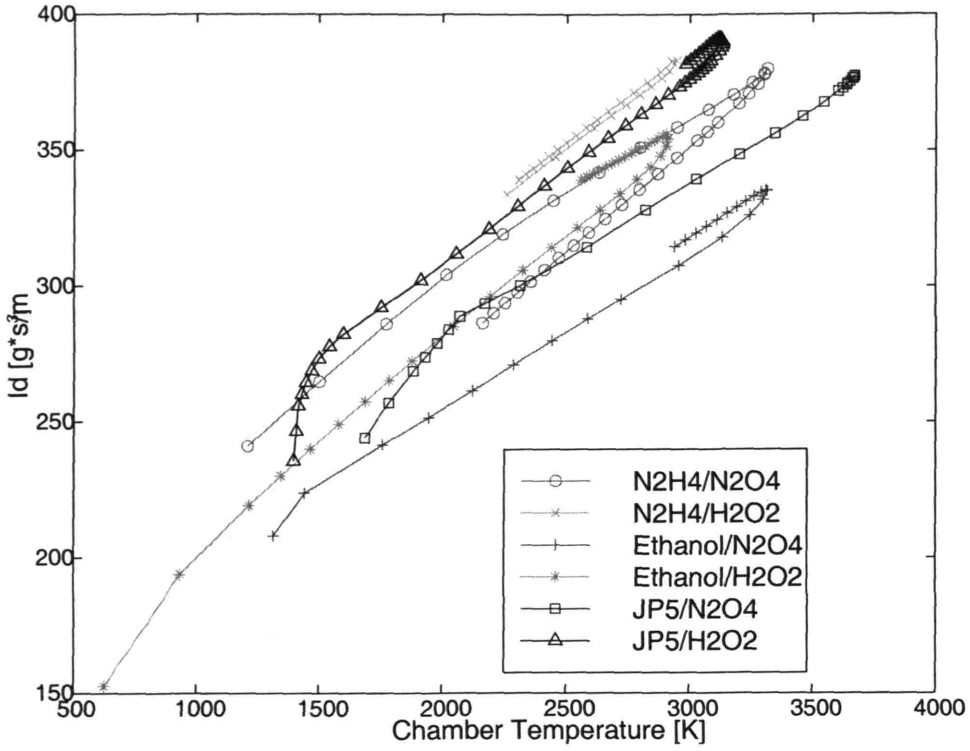

Figure A-4: Density Specific Impulse vs. Chamber Temperature of Selected Propellant Combinations Assuming Chemical Equilibrium.

BIBLIOGRAPHY

Anderson, W. et al. "Low Cost Propulsion Using a High Density, Storable, and Clean Propellant Combination." AIAA/ASME/SAE/ASEE Joint Propulsion Conference & Exhibit, 34th, Cleveland, OH, July 13-15, 1998.

Al-Midani, O. M. "Preliminary Design of a Liquid Bipropellant Microfabricated Rocket Engine." Master's thesis, MIT, May 1998.

Barin, I. *Thermochemical Data of Pure Substances.* 3rd ed. VCH Publishers, Inc., New York, 1995.

Deux, A. Personal Communications, 2000.

Edwards, T. and Eitman, D. A. "Evaluation of Heat Transfer and Thermal Stability of Supercritical JP-7 Fuel." 33rd AIAA/ASME/ASEE Joint Propulsion Conference and Exhibit, Seattle, WA, July 6-9, 1997.

Epstein, A. H., et al. "The MIT Microengine Project, 1998 Annual Technical Report, MIT Proprietary, Cambridge, MA, 1998.

FMC. Hydrogen Peroxide Physical Properties Data Book. 2nd ed. Food Machinery and Chemical Corporation Becco Chemical Division. Buffalo, New York, 1955.

Francis, R. "A Systems Study of Very Small Launch Vehicles." Master's thesis, MIT, September 1999.

Franz, A. 1998. Personal Communications.

Green, D. "Modified Oxides of Nitrogen-III (MON-III_ - Nitrogen Tetroxide Material Safety Data Sheet (MSDS)." Vicksburg Chemical, Vicksburg, MS, 1993.

Gordon, S. and McBride, B. J. Computer Program for Calculation of Complex Chemical Equilibrium Compositions and Applications. NASA Reference Publication 1311. October 1994.

Hamrock, B. J. Fundamentals of Fluid Film Lubrication. McGraw-Hill, Inc., 1994.

Haws, J. W. et al. "Thermodynamic Properties of Hydrazine." Journal of Spacecraft. Vol. 2, No. 6. November-December 1965.

Hill, P. G. and Peterson, C. R. *Mechanics and Thermodynamics of Propulsion.* 2nd ed. Addison-Wesley, Reading, MA, 1992.

Jacobsen, S. Personal Communications, 1999.

Kakac, S. et al. Handbook of Single-Phase Convective Heat Transfer. John Wiley and Sons, Inc., New York, 1987.

Kerrebrock, J. L. Aircraft Engines and Gas Turbines, 2ed. The MIT Press, Cambridge, MA, 1992.

Kerrebrock, J. L. Personal Communications, 1999.

Lohner, K. A. "Microfabricated Refractory Ceramic Structures for Micro Turbomachinery." Master's thesis, MIT, June 1999.

London, A. P. "A System Study of Propulsion Technologies for Orbit and Attitude Control for Microspacecraft." Master's thesis, MIT, May 1996.

London, A. P. Personal Communications regarding on-going research for MIT Ph. D. thesis tentatively titled, "Development and Test of a Microfabricated Bipropellant Rocket Engine," 1999.

Manski, D. et al. "Cycles for Earth-to-Orbit Propulsion." Journal of Propulsion and Power. Vol. 14, No. 5. September-October 1998.

McCormick, J. C. "Hydrogen Peroxide Rocket Manual." FMC Corporation. 1965.

Mehregany, M. and Senturia, S. D. "Anisotropic Etching of Silicon in Hydrazine." Sensors and Actuators, 13, 1998.

Pillori, G. L. "Material Safety Data Sheet (MSDS) for Anhydrous Hydrazine." Fisher Scientific Chemical Division. Fair Lawn, NJ, 1988.

Primex. *Hydrazine Handbook.* Primex Aerospace Company. Redmond, WA, 1997.

Senturia, S. D. Personal Communications, 1999.

Shell Chemical Company. "Concentrated Hydrogen Peroxide, H2O2, Properties Uses Storage, Handling." 2nd ed. Shell Chemical Company Industrial Chemicals Division. 1962.

Stai, D. F. et al. "Thermodynamic Properties of Nitrogen Tetroxide." Journal of Spacecraft. Vol. 2, No. 5. September-October 1965.

Sutton, G. P. Rocket Propulsion Elements, 6 ed. John Wiley and Sons, Inc., New York, 1992.

Schmidt, E. W. Hydrazine and its Derivatives : Preparation, Properties, Applications. J. Wiley, New York, 1984.

USAF. *USAF Propellant Handbooks, Nitric Acid/Nitrogen Tetroxide Oxidizers.* Martin Marietta, 1977.